ORGANIC CHEMISTRY FRONTIERS

REVIEW

View Article Online
View Journal | View Issue

Cite this: *Org. Chem. Front.*, 2020, **7**, 3530

Recent advances in transition metal migration involving reactions

Xu Dong,†[a] Hui Wang,†[b] Hui Liu *[a] and Fagang Wang*[a]

Received 12th May 2020,
Accepted 27th August 2020

DOI: 10.1039/d0qo00558d

rsc.li/frontiers-organic

Numerous elegant methodologies involving transition-metal migration processes have received increasing attention and they have gradually developed into significant synthetic tools in the past few decades. These strategies provide novel ways to build a carbon–metal bond at a new position, where it may not be facile or straightforward to introduce a metal atom. Hence, metal-migration reactions exhibit attractive practicability in synthetic organic chemistry. This review gives an up-to-date overview of catalytic methodologies involving metal-migration processes, which are sorted into categories such as 1,2- to 1,5- and 1,7-Pd migration, 1,3- to 1,5-Rh migration, 1,4- and 1,5-Fe migration, and so on. For most of these transformations, plausible mechanisms are demonstrated elaborately. Clarification of these processes is a key point for understanding metal-migration involving reactions and developing new high-performance methodologies.

1 Introduction

Transition-metal-catalyzed reactions have emerged as powerful alternatives to versatile functionalized molecules. Most importantly, significant progress has been witnessed in reactions for the construction of carbon–carbon and carbon–heteroatom bonds, exhibiting advantages of improved atom- and step-economy compared to conventional methods.[1] Generally, carbon–metal bonds can be generated *via* oxidative addition, transmetalation, insertion into unsaturated bonds, C–H bond activation, and so on. However, it is not easy to introduce a metal moiety into a specific position of an organic molecular skeleton. Recently, the metal-migration process has shown attractive applications to form unique carbon–metal bonds, and they could be transformed into valuable compounds that otherwise would be difficult to achieve *via* classic processes. Palladium catalysis, as one of the most important synthetic tools in modern organic synthesis, shows a special application in the synthesis of complicated molecules *via* a controllable migration and remote C–H activation strategy. In 2005, Ma *et al.* contributed a prospective review on the elementary art of including 1,4-migration of palladium.[2] In 2010, the Larock group summarized the reactions of 1,4 and 1,5-migration of palladium.[3] Very recently, Gu *et al.* provided a comprehensive review on 1,4-migration of transition metals in organic synthesis, including palladium-catalyzed strategies.[4] With the development of palladium chemistry, palladium migration became a quite unique tool in organic synthesis based on ready design and control. More and more novel transformations, involving 1,2- to 1,5- and 1,7-palladium migration, have emerged dramatically. Additionally, Rh, Fe, Co, Ir, Cr, Ni, and Pt also demonstrate appealing migratory behaviors in synthetic chemistry. Herein, this review mainly summarizes the metal-migration reactions in the past nearly 20 years, including elaborate mechanism presentation, hoping to give a preliminary understanding of this field for the chemists in need.

2 Palladium migration

2.1 1,2-Palladium migration

As illustrated in Scheme 1, 1,2-palladium migration occurs *via* sequential β-H elimination and hydropalladation processes in most cases. This elimination/reinsertion process frequently occurs in Heck type reactions, especially the migration of olefins, and chemists differ in their attitudes towards the process of reversible β-hydride elimination/reinsertion, which might not be considered and classified as a 1,2-palladium

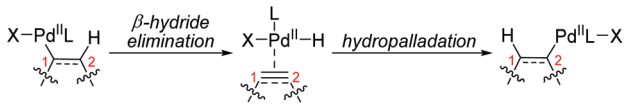

Scheme 1 Proposed process of 1,2-palladium migration.

[a]*School of Chemistry and Chemical Engineering, Shandong University of Technology, 266 West Xincun Road, Zibo 255049, China. E-mail: huiliu1030@163.com, a_gang@sdut.edu.cn*
[b]*Shandong Jincheng Kerui Chemical Co., Ltd., Zibo 255100, P.R. China*
†These authors contributed equally.

migration process. Hence in this section, only a few typical examples, classified as 1,2-Pd migration by the original authors, are exhibited to give a preliminary understanding for those unfamiliar with this field. More examples toward elimination/reinsertion processes can be found in metal chain walking research.[5]

The affecting factors and dynamics of 1,2-palladium migration are mainly associated with steric hindrance and the stability of the intermediate. The details will be described in the following reaction examples.

In 2006, a 1,2-migration involved palladium-catalyzed Negishi coupling was described by the Skrydstrup group (Scheme 2).[6] The highest selectivity of 1,2-migration was achieved *via* employing Josiphos ligands with neither electron-donating nor -withdrawing substituents on the phenyl ring. The ratio of rearranged/normal products was up to 19 : 1 with the combination of $Pd(dba)_2$ and PPF-*t*-Bu. The employment of electron-deficient aryl zinc reagent seemed to favor this migratory process, such as **3b**. Further exploration experiments toward more nucleophilic aryl Grignard reagents revealed that the nucleophilicity of the organometallic reagents might influence the competition between the transmetalation step and the intermediate-hydride elimination of the alkenyl Pd(II) species (Scheme 3). The pathways illustrated in Scheme 4 better visualize this process. The ligand based Pd(II) intermediate **9** would furnish the non-migratory products **10** in cases where the transmetalation was fast (path A), otherwise a ligand dissociation might take place to form a trigonally coordinated palladium(II) complex **11** possessing a vacant site (path B). Sequential β-hydride elimination in vinyl (**12**) and hydropalladation afforded the migrated vinylic Pd(II) compound **13**, which finally provided the migratory products **14**.

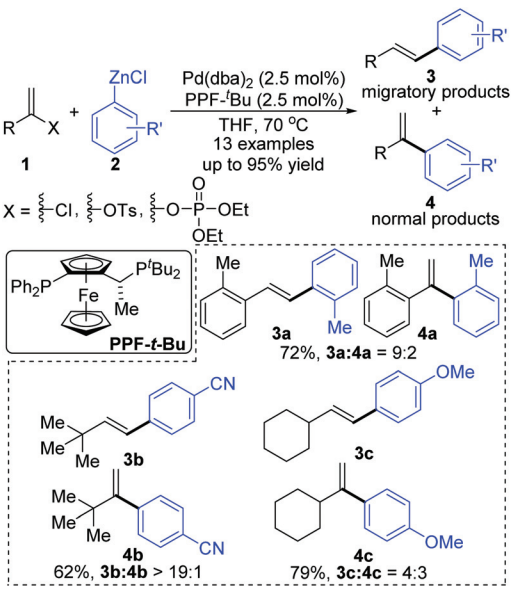

Scheme 2 Skrydstrup's Negishi couplings involving a 1,2-palladium migration process.

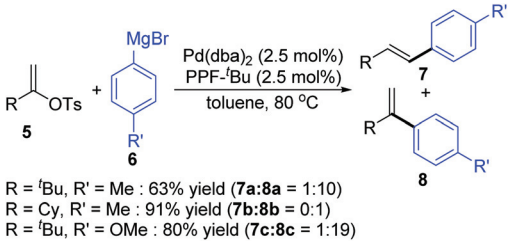

Scheme 3 Exploration experiments involving Grignard reagents with 1,2-migration.

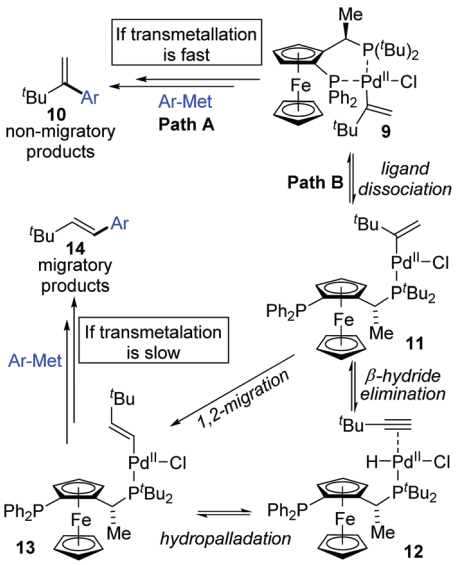

Scheme 4 Different reaction pathways based on the nucleophilicity of the organometallic reagents.

Then, Skrydstrup *et al.* further reported 1,2-palladium migration involved studies toward Heck reaction with alkenyl phosphates **15** (Scheme 5).[7] The employment of X-Phos and excessive LiCl (10 equiv.) could suppress 1,2-migration efficiently to give the normal products **17**, while ligand $HBF_4P(t\text{-}Bu)_3$ tended to encourage the migratory products **18**. Studies also showed that the 1,2-migration was largely dependent on the C1-substituent, and high migratory selectivity was observed for substrates bearing a C1-alkyl quaternary carbon, such as product **18a**. However, the perfluorophenyl vinyl phosphate afforded the non-migratory product **17d** in a high yield under condition B, indicating that electronic factors held important implications for this transformation. The possible 1,2-palladium migration was revealed in Scheme 6. Initial oxidative addition of Pd(0) afforded a tri-coordinated Pd(II) intermediate **19** possessing a free site on the palladium for the following β-elimination step. And this elimination step was sensitive to the steric hindrance, which could prevent interaction of the metal center with the vinylic hydrogen. Just as condition A offered the non-migratory products exclusively by using the sterically hindered ligand X-Phos, with condition B, the hydro-

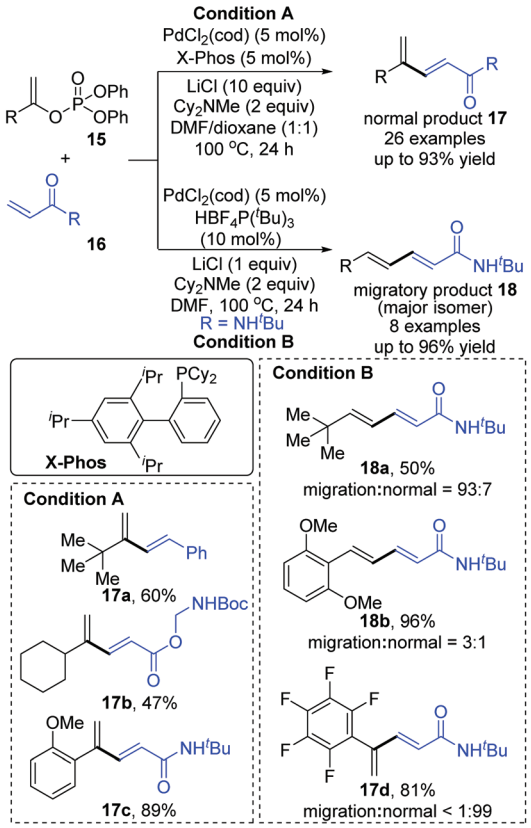

Scheme 5 Skrydstrup's Heck-type reactions involving 1,2-migration.

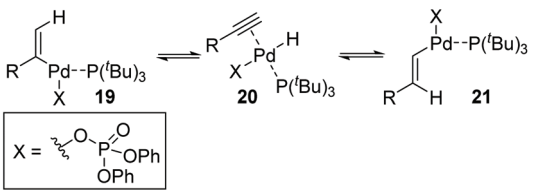

Scheme 6 Possible mechanism for 1,2-Pd migration in Heck reactions.

palladation of intermediate **20** allowed the Pd(II) group to move to the uncrowded vinyl-terminal and form the migratory Pd(II) complex **21**.

In 2016, Gulevskaya and co-workers reported a palladium-catalyzed reaction to synthesize a series of alkynyl derivatives of 1,3-dialkylperimidones.[8] A previously unknown 1,2-migration of the Pd(II) group on the phenyl ring was observed when they dealt with the coupling of tetrabromide **22** with trimethylsilylacetylene (Scheme 7). Presumably, the formation of **26** originated from the 1,2-shift of the Pd(II) group in either intermediate **23a** or **23b**. And the motive force for such a migration should come from the harsh steric tension; therefore the PdBr group looked more likely to go through this migration. Inspired by 1,2-migrations in the Pd(II) alkenyl complexes,[7a] an aryne intermediate **24a** was supposed to be generated *via* β-hydride elimination. The subsequent regioselective hydropalladation would furnish the migratory aryl palladium

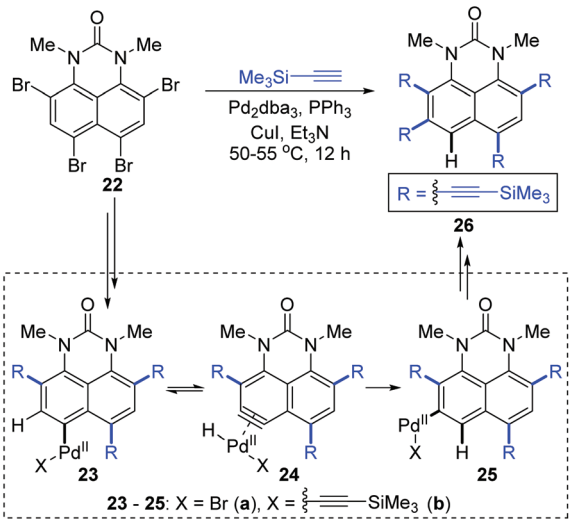

Scheme 7 An example of 1,2-Pd migration in Sonogashira coupling.

species **25a**, which afforded the final product **26** *via* Sonogashira coupling reaction.

Later, a synthetic method for the preparation of 2-arylindoles involving a 1,2-palladium migration process was reported by the Yue group (Scheme 8).[9] A series of 2-arylindoles **29** were obtained in moderate to high yields *via* Suzuki coupling reaction of 3-bromoindoles **27** with hindered boronic acid **28** catalyzed by $Pd(OAc)_2/PCy_3$. The steric hinderance of mesitylboronic acids was very crucial for this 1,2-migration, and no migratory product was observed in the presence of less hindered boronic acids. The basicity of the base also significantly affected the selectivity and yield, and weaker base gave a better performance. The proposed catalytic cycle is shown in Scheme 9. Initially, an aryl-palladium intermediate **30** was generated *in situ via* the oxidative addition of **27** to Pd(0). The sequential "oxo-palladium" pathway and transmetalation deli-

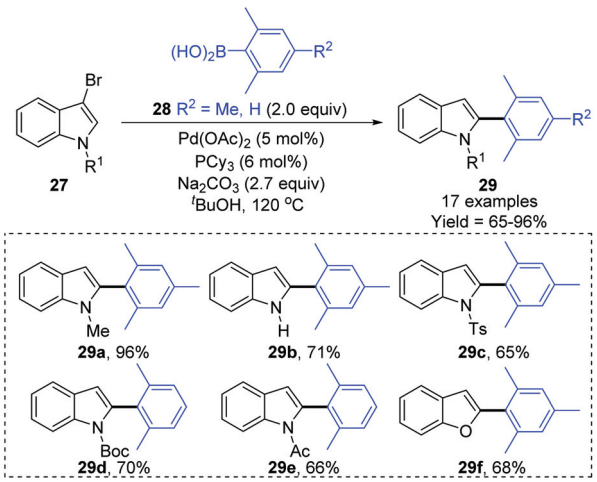

Scheme 8 Yue's 1,2-Pd migration strategy in the Suzuki coupling of indoles.

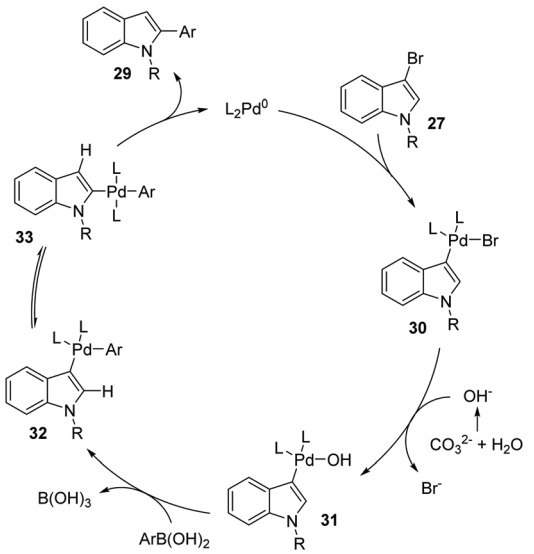

Scheme 9 Proposed mechanism for the Suzuki coupling of indoles *via* 1,2-Pd migration.

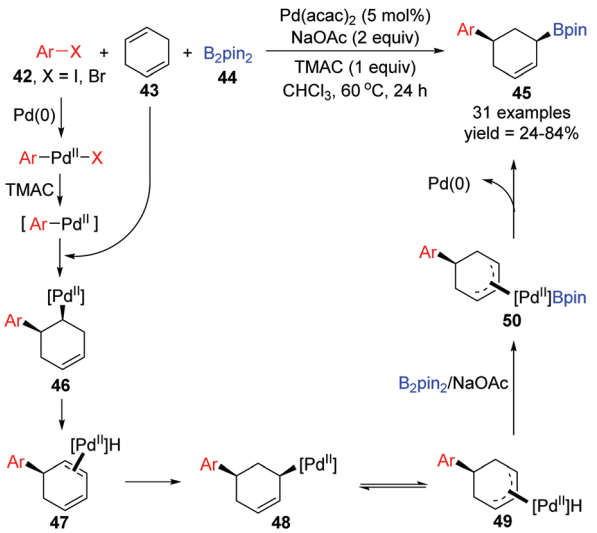

Scheme 11 Palladium-catalyzed 1,3-arylboration of unconjugated dienes.

vered the intermediate **32**, which was compelled to undergo 1,2-palladium migration due to the effect of the aryl steric hindrance and the ligand. Finally, the reductive elimination of the thermodynamically more stable 2-palladium species **33** afforded the 1,2-migrated products **29**.

Moreover, a possible 1,2-palladium migration is also observed in the work of the Fleischer group.[10] As shown in Scheme 10, a tandem olefin migration/hydrothiolation of allyl benzenes was achieved, which was facilitated by an *in situ* generated palladium hydride **37**. In the proposed catalytic cycle, a 1,2-palladium migration could take place from intermediate

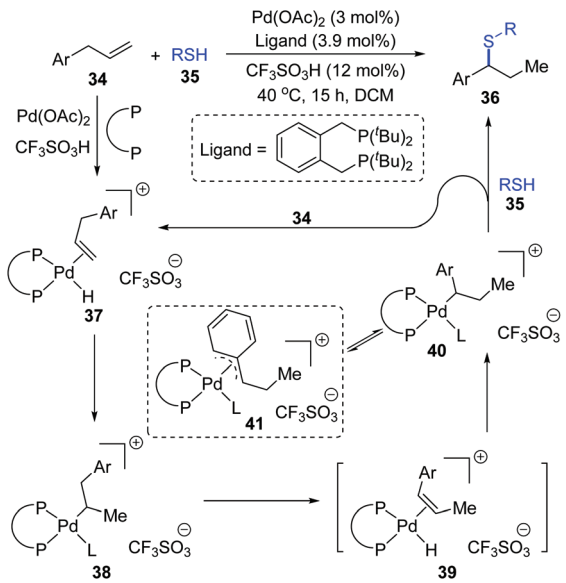

Scheme 10 Hydrothiolation of allyl benzenes *via* 1,2-palladium migration.

38 to **40** *via* the elimination/coordination/insertion sequence. The more stable η^3-coordination mode of species **41** might be responsible for the migratory motivation. In this procedure, coordination of thiol to a palladium atom (L in **38**, **40**, and **41**) might occur in advance to account for the final formation of a C–S bond; alternatively, direct substitution between **40** and **35** was also feasible.

Recently, the Yin group achieved a novel palladium-catalyzed arylboration of 1,4-cyclohexadienes **43**, which allowed expedited access to diverse functionalized 1,3-disubstituted cyclohexanes **45** from readily available starting materials (Scheme 11).[11] Notably, this three-component reaction did not rely on the application of dative ligands, but a cheap ammonium chloride salt (TMAC) instead, and the 1,3-difunctional product **45** prepared *via* this protocol possessed exclusive *cis*-diastereoselectivity. In the proposed catalytic cycle, the intermediate Ar–Pd^{II}–X, generated from oxidative addition of aryl halides **42** with Pd(0), would further transform into a new Pd(II) species Ar–Pd^{II} in the presence of TMAC, which was inserted by 1,4-cyclohexadienes **43** to afford intermediate **46**. Then the intermediate **46** rapidly underwent β-H elimination and migratory insertion. The excellent stereoselectivity observed in the products revealed that the Pd–H did not dissociate from the substrate **47** in this process. It seemed that the migratory force could be explained by a more stable π-allylPd(II) intermediate **49**. Finally, sequential transmetalation with B_2pin_2 and reductive elimination gave the target products **45**.

2.2 1,3-Palladium migration

So far, transformation involving 1,3-palladium migration is just an emerging research project in the field of metal migration, and the relevant mechanism study is still in its infancy. Hence the elaborate mechanisms of 1,3-palladium migration are not well explored. Based on the current reports,

structures of allyl palladium seem to be significant for the 1,3-migration, so it can be speculated that the Pd-migration may proceed *via* an intermediate **52** similar to π-allylpalladium (Scheme 12). However, there is no concrete evidence to prove this process, and further mechanism investigation experiments are essential. Moreover, several existing examples proposed as 1,3-Pd shifts seem to be indistinguishable with the π-allylic palladium chemistry, such as the following first example. Therefore, getting direct evidence for defining a 1,3-palladium migration involved strategy is another imperative in future research.

In 2011, Studer and co-workers developed a palladium-catalyzed coupling of 2,5-cyclohexadiene-1-carboxylic acid derivatives with aryl iodides, achieving stereoselective $C(sp^3)$–$C(sp^2)$ bond formation (Scheme 13).[12] Chiral substrates **54** were converted into the corresponding dienes **55** stereospecifically, while racemic products **57** were obtained from achiral substrates **56**. The steric hindrance of the R group has a significant effect on this transformation. For instance, substrates possessing isopropyl groups (R = i-Pr) with larger steric hindrance than the ethyl group (R = Et) afforded the corresponding products in higher yield (**57a** and **57b**). When an additional methyl group was installed at either the 2- or 3-position of the substrate **56**, palladium migration took place preferentially on the side of the olefin without substituent (**57c** and **57d**). However, the 2,5-dimethyl substrate **58** did not give the

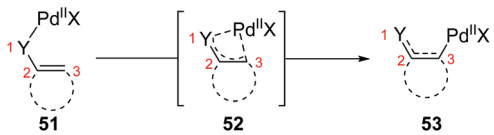

Scheme 12 Possible procedure of 1,3-palladium migration.

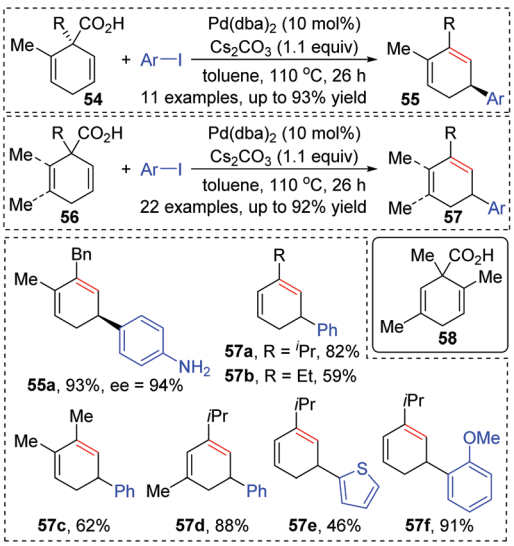

Scheme 13 Pd-Catalyzed coupling of 2,5-cyclohexadiene-1-carboxylic acid derivatives with aryl iodides.

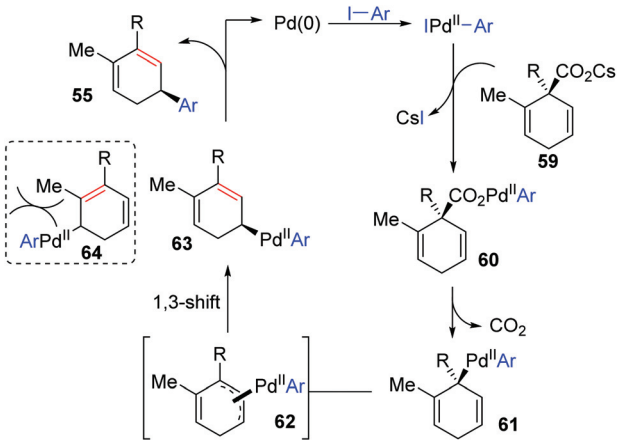

Scheme 14 Suggested mechanism for the reaction of 2,5-cyclohexadiene-1-carboxylic acids with aryl iodides.

corresponding product due to steric reasons. The proposed catalytic cycle is illustrated in Scheme 14. Taking chiral substrates **54** as an example, I–Pd(II)–Ar species were generated *via* oxidative addition of aryl iodide to Pd(0). Then ligand exchange between I–Pd(II)–Ar and cesium salt **59** could form intermediate **60**, which further provided 2,5-cyclohexadienyl palladium species **61** with retention of stereochemistry *via* a decarboxylation process. Stereospecific 1,3-Pd migration *via* a π-allylpalladium intermediate **62** delivered the migratory species **63**. Final reductive elimination led to target chiral product **55** with the release of Pd(0). Additionally, the existence of regioisomeric intermediate **64** could not be entirely excluded; however, intramolecular tension makes it hard to compete with **63**. Furthermore, even if the intermediate **64** is generated, it is more likely to reconvert into **63** *via* a 1,3-shift process.

In 2015, a 1,3-palladium migration involved novel synthetic methodology for preparing 4-aminoquinoline derivatives **67** was reported by the Wang and Ji group (Scheme 15).[13] This protocol employed diverse enaminones **65** and isocyanides **66** as the reaction substrates to give the corresponding products in moderate yields, while the annulation did not take place with enaminones bearing a strong electron-withdrawing group in the benzene ring, such as nitro. On the basis of exploration experiments, a plausible reaction mechanism was proposed for this 1,3-migration process (Scheme 16). Initial ligand exchange between Pd(dppf)$_2$Cl$_2$ and isocyanide **66** generated a bis(isocyanide)palladium(II) complex **68**. Subsequent addition of enaminones **65** to complex **68** afforded the Pd(II) intermediate **69** with a five-membered ring transition structure. Then, a seven-membered palladacycle **70** was furnished *via* 1,3-Pd shift from the amine to the adjacent aryl C–H bond. And the results of the kinetic isotope effect revealed that the cleavage of the aryl C–H bond by 1,3-palladium migration is not the rate-determining step. Subsequent reductive elimination led to the acidic intermediate **71**, which was unstable and converted into the desired cyclization product **67** rapidly under basic con-

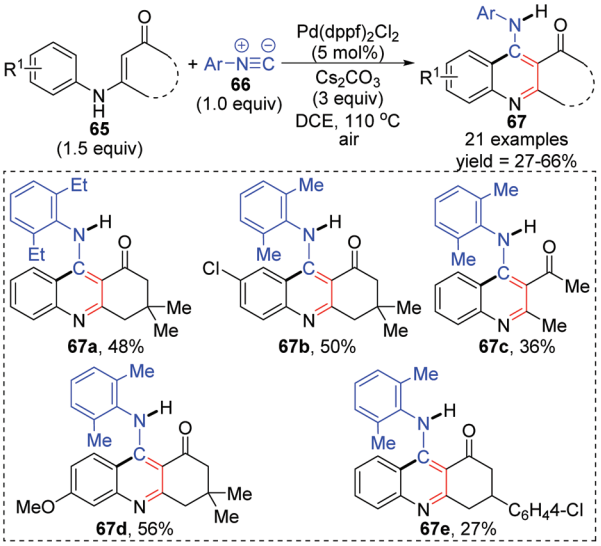

Scheme 15 Synthesis of 4-aminoquinoline derivatives *via* 1,3-palladium migration.

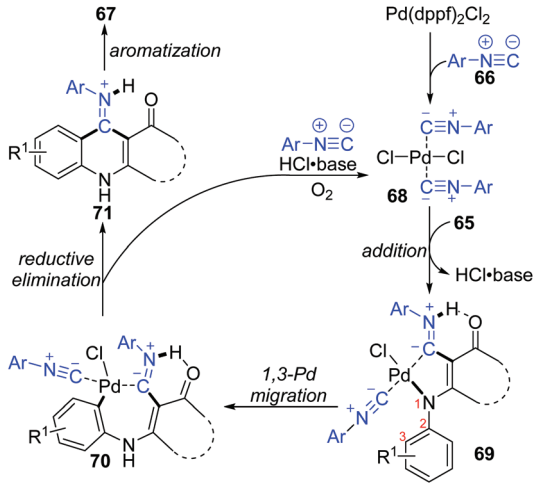

Scheme 16 Possible mechanism for preparing 4-aminoquinolines from enaminones and isocyanides.

ditions *via* aromatization. The activated Pd(II) species **68** was regenerated by air oxidation in the presence of hydrochloride and isocyanide simultaneously.

An interesting 1,3-palladium migration process was also observed in Wang's strategy of synthesizing imine derivatives *via* dearomatization reaction of *N*-aryl ureas with internal alkynes.[14] The Pd-migration occurred when 2-naphthyl ureas **72** were employed as the substrates, and a proposed catalytic pathway to shed light on the migrated product formation is illustrated in Scheme 17. Based on the primary mechanism investigations, an intermediate **75** should be generated preferentially from electrophilic attack of the directing-group-coordinated $Pd(OAc)_2$ to the 3-position of 2-naphthyl urea **72**. The sequential 1,3-shift of the Pd center generated intermediate **76**, which was probably thermodynamically more stable due to the stabilization of the C–Pd bond with an adjacent phenyl group. Intermediates **77** and **78** were afforded *via* migratory insertion of alkyne **73**. Allyl sp^3 C–H olefination of **78** delivered the spirocyclic compound **79**, accompanied by Pd(0) release. The final migrated product **74** was generated by deprotonation of **79**.

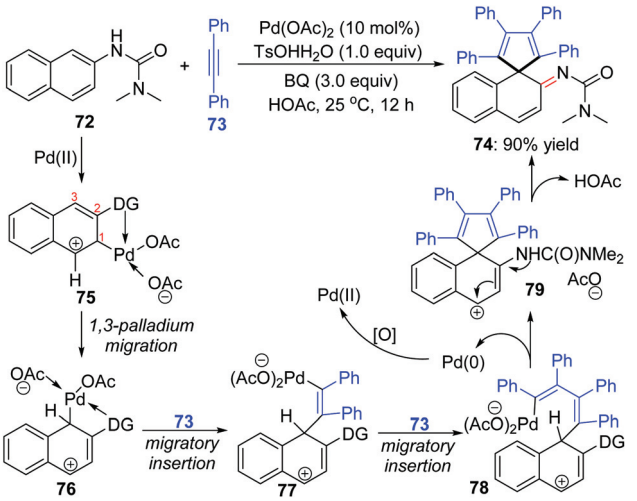

Scheme 17 1,3-Palladium migration in synthesizing imine derivatives.

In 2019, the Liang group reported a three-component cross-coupling of *o*-iodoaniline **80**, *N*-benzoyloxyamines **81**, and norbornadiene **82** to access highly functionalized 4-aminoindoles **83** (Scheme 18).[15] The Catellani and retro-Diels–Alder strategy was employed in this domino process. And this method also

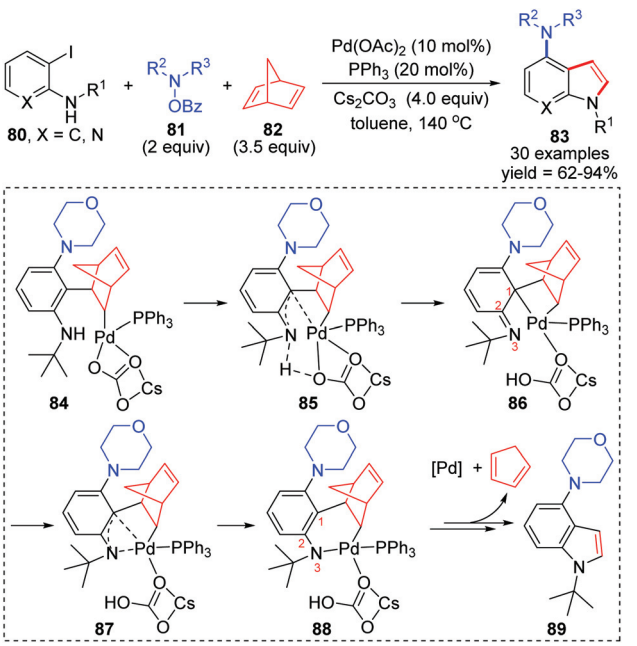

Scheme 18 1,3-Palladium migration that occurred in intramolecular Buchwald coupling.

exhibited good industrialization potential by a gram-scale reaction investigation (79% yield of isolated product). On the basis of density functional theory calculations, the authors pointed out that a 1,3-palladium migration process should be involved in the intramolecular Buchwald coupling of this reaction. Details are also illustrated in Scheme 18. Firstly, the coordination of benzene with palladium might cause the carbonyl group of the carbonate to leave and generate an imine (from **84** to **86**). Then, 1,3-Pd migration occurred to form intermediate **88** *via* a π-allylicpalladium analogue **87**, which further released the Pd catalyst and 1,3-cyclopentadiene to afford the target product **89**. However, it is important to note that the process from intermediates **84** to **86** was merely proposed according to the computation studies, which was not supported by experimental results. Hence, the subsequent 1,3-Pd migration was only assumed by the authors to rationalize the calculations.

2.3 1,4-Palladium migration

1,4-Palladium migration is the most widely investigated strategy among metal-migration involving reactions (Scheme 19). Due to its relatively stable transition state of a five-membered ring, such as species **91**, **92**, and **93**, 1,4-palladium migration is quite common in organometallic chemistry compared with other migratory types. The strategy of 1,4-migration can be widely used to metalate a remote C–H bond, generating a new organometallic species that is difficult to achieve by other conventional approaches. Numerous elegant methodologies involving various types of 1,4-palladium migrations, such as aryl-to-vinyl, vinyl-to-aryl, aryl-to-aryl, aryl-to-benzyl *etc*., have been developed over the past decade. In this section, only complementary reports are summarized according to the previously reported reviews;[2–4] more strategies toward 1,4-Pd migration can be found in the referenced literature.

2.3.1 Aryl-to-vinyl 1,4-palladium migration. In early 2020, the Yu and Zhou group achieved a Pd-catalyzed C–H alkylation of gemdisubstituted ethylenes **95** *via* an aryl to vinyl 1,4-palladium migration/ring-opening C–C cleavage process (Scheme 20).[16] The trisubstituted alkenes **97** were afforded in high yields with good regioselectivity, broad substrate scopes, and good functional group tolerance. An elaborate catalytic cycle, proposed based on mechanistic study and DFT calculations, is illustrated in Scheme 28. After oxidative addition of Pd(0) to the C–Br bond (**95**), a subsequent 1,4-palladium migration process occurred from the aryl to vinyl position *via* an intermolecular hydrogen atom transfer (**101** to **104**).

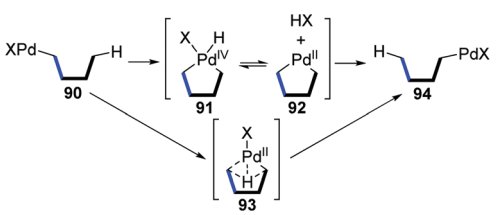

Scheme 19 Possible transition state of 1,4-palladium migration.

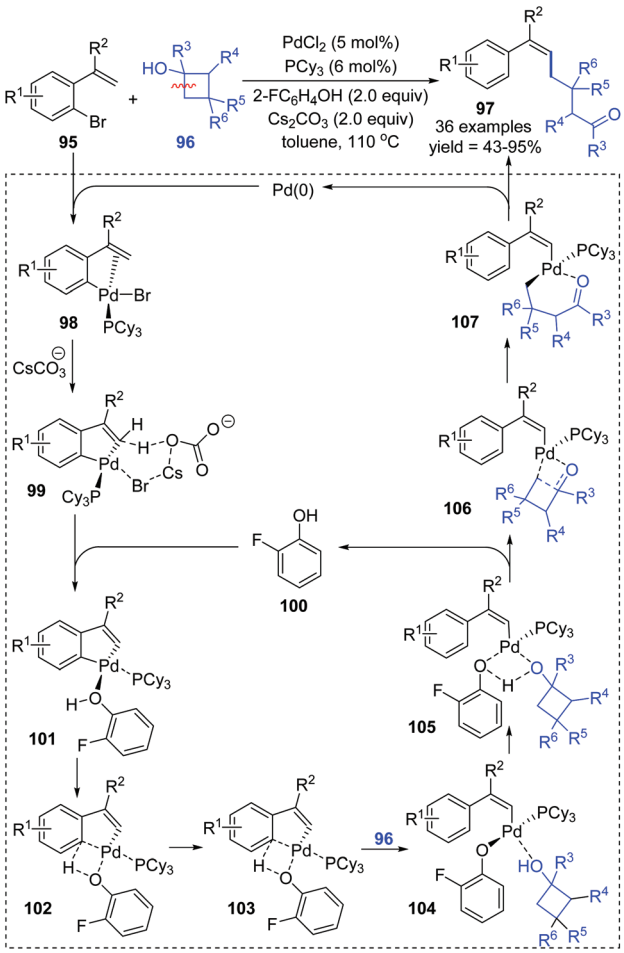

Scheme 20 Pd-Catalyzed coupling reaction *via* an aryl to vinyl 1,4-palladium migration/ring-opening C–C cleavage process.

Coordination of cyclobutanol **104** to the palladium center caused its hydroxyl hydrogen to shift to the 2-F-phenoxy functionality, readily removing 2-FC_6H_4OH from the metal center (**105** to **106**). Then, a ring-opening C–C cleavage process of **106** afforded the thermally stable intermediate **107**, which further delivered the final product **97** by reductive elimination.

Very recently, a novel Suzuki–Miyaura coupling enabled by aryl to vinyl 1,4-palladium migration was achieved by the Feng and Lin group (Scheme 21).[17] Diverse stereo-defined multisubstituted olefins **111** were synthesized from coupling of *ortho*-vinyl bromobenzene **109** with aryl/heteroaryl boronate esters **110**. On the other hand, *ortho*-vinyl bromobenzene **109** also reacted with alkenyl boron reagents **112** to prepare a series of 1,3-dienes **113** efficiently. Good yields, broad substrate scope, and excellent functional-group tolerance were observed in these transformations. The tentative catalytic cycle is proposed in Scheme 29. The exchange of the bromide anion with $PivO^-$ occurred to aryl-Pd(II)Br intermediate **114** to form a new Pd(II) species **115**. Then, the following C–H activation energetically favored a five-membered palladacycle(II) **116** *via* a concerted metalation–deprotonation mechanism. Subsequent proton

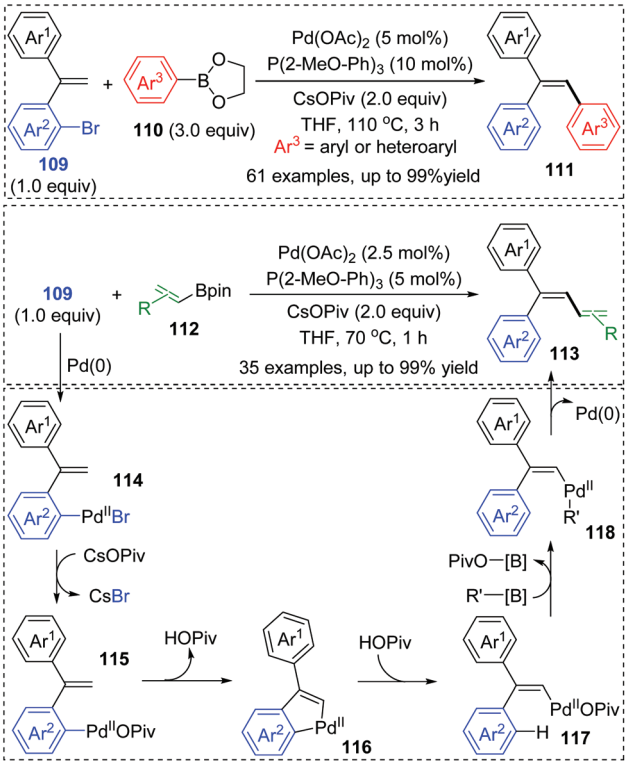

Scheme 21 Pd-Catalyzed Suzuki–Miyaura coupling *via* aryl to vinyl 1,4-palladium migration.

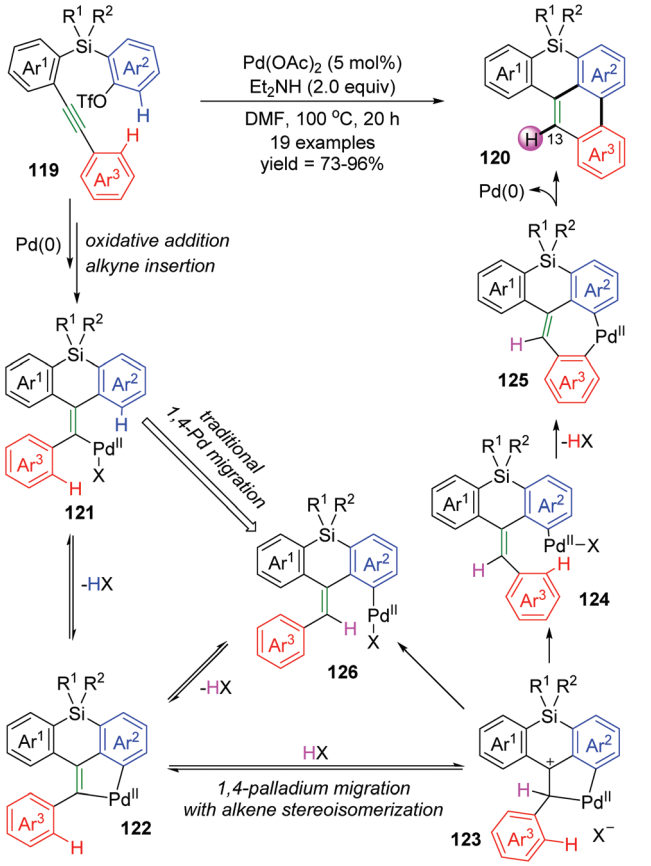

Scheme 22 Shintani's 1,4-Pd migration with concomitant alkene stereoisomerization.

transfer with the aid of HOPiv delivered the palladium-migratory species **117**, which further underwent transmetalation with organoboron reagents to furnish intermediate **118**. Final reductive elimination led to the target product **111** or **113** and regeneration of Pd(0).

2.3.2 Vinyl-to-aryl 1,4-palladium migration. According to the current reports, vinyl to aryl 1,4-Pd migration usually occurs to a vinyl palladium intermediate formed *in situ via* insertion of a C–Pd bond into an alkyne. Similar to other 1,4-Pd shifts, the metathesis between the C(sp^2)–Pd bond of the vinyl and C(sp^2)–H bond of the aryl also takes place *via* a five-membered transition state.

Recently, Shintani and co-workers developed a Pd-catalyzed intramolecular cyclization to prepare 8*H*-benzo[*e*]phenanthro[1,10-*bc*]silanes **120** from easily accessible 2-((2-(arylethynyl)aryl)silyl)aryl triflates **119** under simple reaction conditions.[18] As shown in Scheme 22, two C–H bonds on Ar^2 and Ar^3 of substrate **119** were cleaved to form a C–C bond between the two rings, and a new C–H bond was generated at the 13-position of the resulting product **120**. However, several deuterium-labelling experiments revealed that the H atom at the 13-position was derived from an external hydrogen donor (Et_2NH and/or residual water in the solvent) instead of the Ar^2 group. According to these results, a new mode of 1,4-palladium migration involving concomitant alkene stereoisomerization was preliminarily established as illustrated in Scheme 22. Initial successive oxidative addition of aryl triflate **119** to palladium(0) and insertion of alkyne generated the alkenylpalladium **121**. Then, C–H bond activation on Ar^2 led to a five-membered palladacycle **122**, which underwent protonation by an external proton donor to form a cationic species **123**. Subsequent cleavage of the alkyl–Pd bond with accompanying formation of a *Z* alkene afforded the key intermediate **124**, which could further undergo C–H bond activation to generate a seven-membered palladacycle **125**. Final reductive elimination gave the target product **120**, and regenerated the Pd(0) catalyst. Nevertheless, the traditional 1,4-palladium migratory product **126** could not be excluded for the catalytic cycle.

2.3.3 Alkyl-to-aryl 1,4-palladium migration. The Wang and Ji group achieved a palladium-catalyzed strategy for the synthesis of dihydroindeno [1,2,3-*kl*]acridine derivatives **128** (Scheme 23).[19] The reaction afforded a five-membered ring and six-membered ring simultaneously *via* a 1,4-palladium migration process. Two regioisomers could be produced, while there were substituents on the rings B or C, such as **128b** and **128b′**. A possible reaction pathway is illustrated in Scheme 24. Successive oxidative addition of **129** to Pd(0) and intramolecular Heck addition afforded species **130**, which could activate the *ortho* aromatic C–H bond on the A, B or C rings. Then, 1,4-palladium migration occurred to provide three regioisomers **131**, **132** or **133**. A six-membered palladacycle **134** or

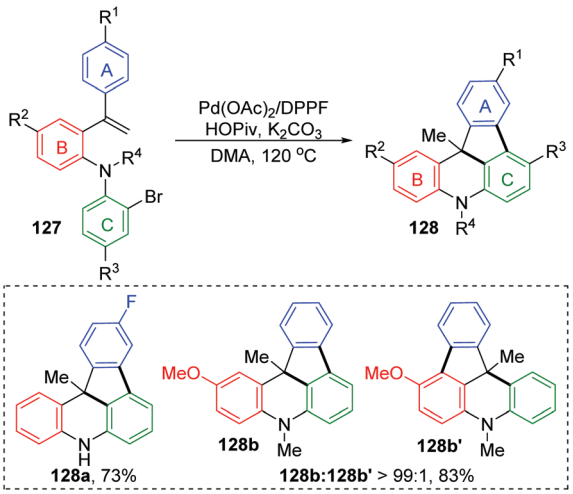

Scheme 23 Pd(0)-Catalyzed reaction for the synthesis of dihydroindeno[1,2,3-*kl*]acridines.

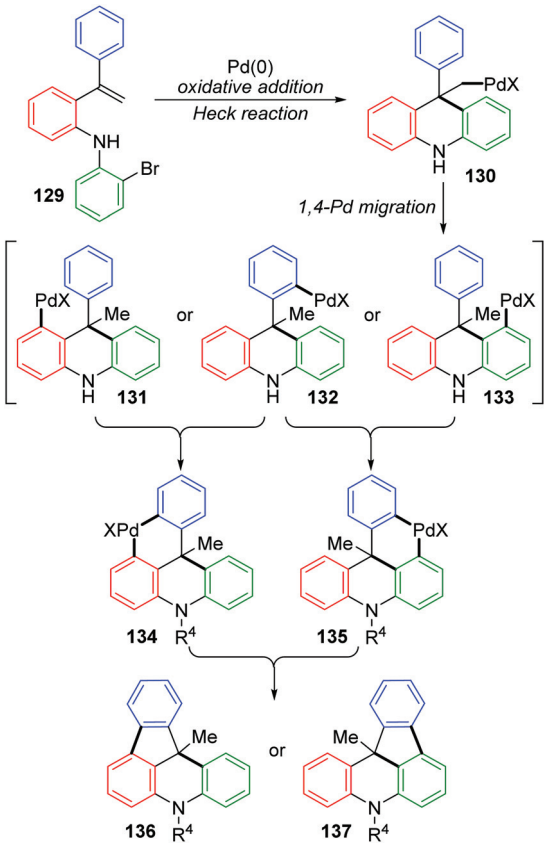

Scheme 24 Plausible mechanism for the Pd-catalyzed synthesis of dihydroindeno[1,2,3-*kl*]acridines.

135 was generated *via* intramolecular cyclization. Finally, the desired products were obtained as a result of reductive elimination, accompanied by reborn Pd(0) catalyst.

For the palladium/norbornene-catalyzed Catellani reaction,[20] it is well-known that multiple types of vicinal functionalized arenes can be achieved *via* the aryl-norbornyl-palladacycle (ANP) intermediate. Recently, Rago and Dong discovered an unexpected *ortho*-Heck reaction *via* 1,4-palladium migration under Catellani reaction conditions (Scheme 25).[21] In the presence of lithium salts, aryl iodide **138** reacted with electron-deficient olefins **139** to furnish the *ortho* Heck products **140** instead of commonly observed *ipso* Heck products **141** in Catellani-type reaction; meanwhile, a norbornyl group was introduced at the *ipso* position of the arene. A possible reaction pathway involving 1,4-Pd migration was proposed according to a series of deuterium labeling studies. Taking deuterated substrate **142** as an example, initial oxidative addition and subsequent norbornene insertion generated the alkyl palladium species **144**, just like the classical Catellani process. However, the 1,4-palladiuim shift took place instead of forming an ANP intermediate to afford the aryl palladium species **146**, accompanied by full transfer of the D atom to norbornene. Results of an isotope crossover experiment also revealed that the 1,4-shift was an intramolecular procedure (**145**), on account of no deuterium exchange between molecules. Finally, the *ortho* Heck product **149** was furnished through a typical Heck reaction pathway; *cis*-migratory insertion (**146** to **148**) and *cis*-β-H elimination (**148** to **149**).

2.3.4 Aryl-to-aryl 1,4-palladium migration. Recently, Lin and Yao *et al.* reported an intramolecular remote C–H activation *via* 1,4-palladium migration, delivering diverse polycyclic frameworks **151** and **153** in moderate to good yields (Scheme 26).[22] The mechanism is similar to that described

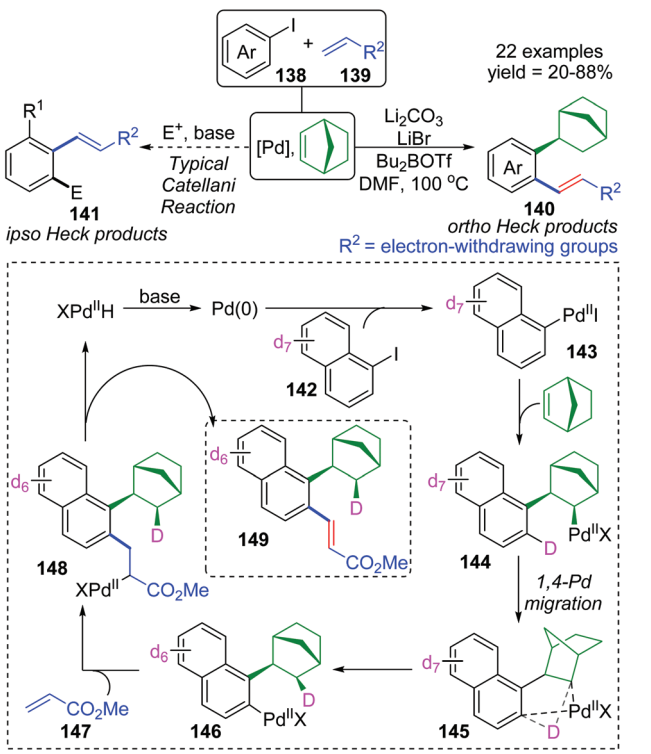

Scheme 25 Palladium/norbornene-catalyzed strategy toward an *ortho*-Heck reaction *versus* a typical Catellani reaction.

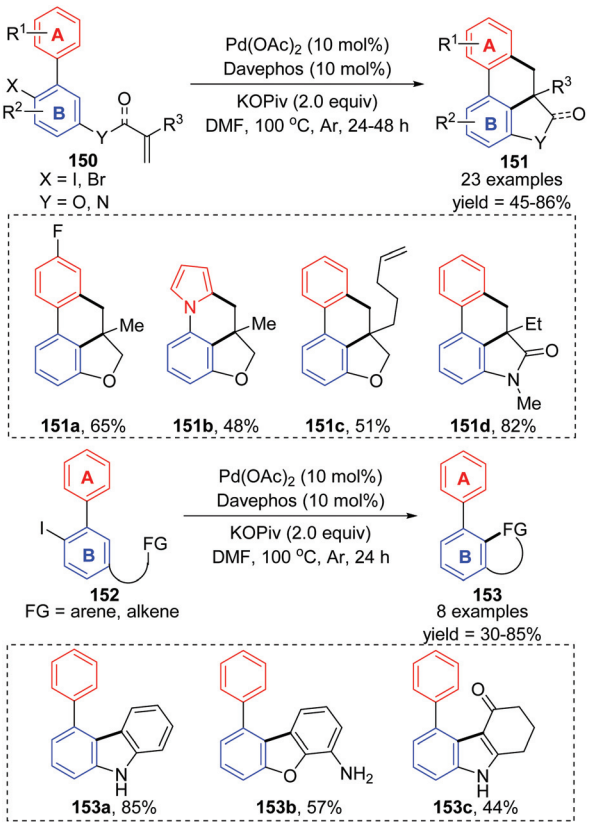

Scheme 26 Preparation of polycyclic frameworks *via* a 1,4-palladium migration pathway.

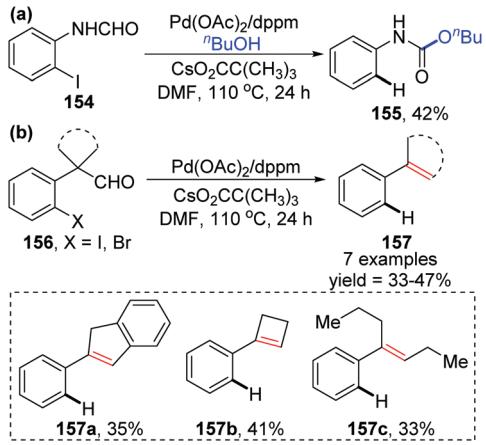

Scheme 27 Pd-Catalyzed strategy for the activation of an acyl C–H bond.

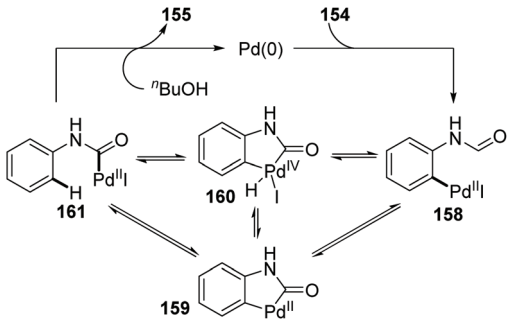

Scheme 28 Proposed catalytic cycle for the synthesis of carbamate.

earlier in this section; successive oxidative addition, twice 1,4-palladium migration between ring A and ring B, alkene insertion, and a C–H activation process were responsible for the final product. Additionally, the authors also pointed out the reversibility of the 1,4-palladium migration between ring A and B.

2.3.5 Aryl-to-acyl 1,4-palladium migration. In 2009, the Larock group reported a novel strategy to activate an acyl C–H bond by employing different aldehydes as substrates, along with a simultaneous palladium shift from the aryl to acyl position (Scheme 27).[23] This transformation offered a carbamate **155** in the presence of nucleophile butanol (Scheme 27a), or a decarbonylation/elimination product **157** in the absence of butanol (Scheme 27b). However, both of the two types of products were obtained in comparatively low yields. A possible reaction mechanism is described in Scheme 28. Taking the formamide **154** as an example, the initial oxidative addition of a carbon–halogen bond to Pd(0) formed an arylpalladium species **158**, which could cyclize to Pd(II) intermediate **159** or further insert into the neighboring acyl C–H bond to afford Pd (IV) intermediate **160**. The migrated acylpalladium species **161** could be generated from either **159** or **160**, and then would be trapped by butanol to provide carbamate **155**. Alternatively, in the absence of a nucleophile, the analogue of **161** would undergo decarbonylation and β-hydride elimination to deliver the Heck-type products **157**.

2.3.6 Aryl-to-alkyl 1,4-palladium migration. In 2019, a novel intramolecular coupling of two C(sp^3)–H bonds *via* 1,4-Pd migration from aryl to alkyl was developed by Baudoin and co-workers (Scheme 29).[24] This reaction proceeded under redox-neutral conditions, with the C–Br bond acting as an internal oxidant. Numerous 2,3-dihydrobenzofurans and indolines **164** were prepared in moderate to good yield (Scheme 29a), and a few 6-membered ring products **166** were also achieved as shown in Scheme 29b. Moreover, in the absence of an enolizable position, the migrated palladium intermediate could attack the ketone to afford a tertiary alcohol **168** (Scheme 29c). However, generally, this transformation is restricted to moderately acidic C–H bonds, adjacent to an oxygen or nitrogen atom on one side and benzylic or adjacent to a carbonyl group on the other side.

2.3.7 Alkyl-to-acyl 1,4-palladium migration. Recently, the Huang and Li group reported a novel strategy for synthesizing diverse lactones *via* a palladium carbene migratory insertion enabled 1,4-palladium migration process (Scheme 30).[25] This protocol achieved a formal dimerization of two readily available reactants, **169** and **170**, providing valuable coupling products medium-sized lactones **171**, which are common structural motifs recurring in many biologically active compounds.

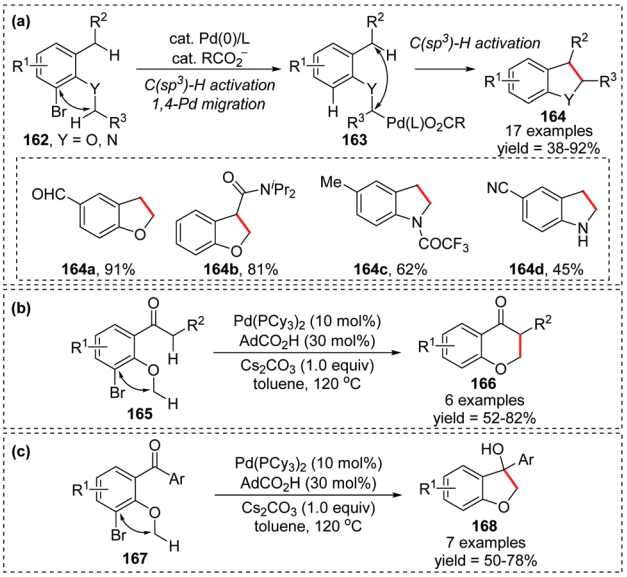

Scheme 29 1,4-Palladium migration assisted C(sp^3)–H/C(sp^3)–H coupling.

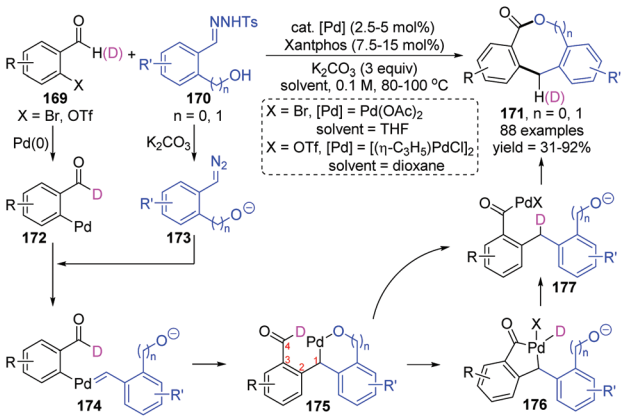

Scheme 30 Synthesis of medium-sized lactones *via* alkyl to acyl 1,4-Pd migration.

Good yield, functional group tolerance, and broad substrate scope were observed in this transformation. A proposed catalytic cycle is also shown in Scheme 30; initial oxidative addition of Pd(0) to *o*-pseudo-halo benzaldehyde **169** formed a Pd(II) intermediate **172**, which further acted as a receptor to react with diazo compound **173**, affording the palladium-carbene intermediate **174**. Subsequent intramolecular migratory insertion of **174** generated a new Pd(II) species **175**. The 1,4-palladium shift from alkyl to acyl could occur directly or *via* a five-membered palladacycle **176**, producing the Pd-migrated intermediate **177**. Final ring closure of **177** generated the target medium-sized lactone **171**.

Shortly afterwards, Huang and co-workers further achieved a palladium-catalyzed formal [4 + 3] annulation for preparing valuable dibenzo-[*b*,*e*]azepin-6-ones **180** from easily accessible *o*-haloarylaldehydes **178** and *N*-tosylhydrazones **179**

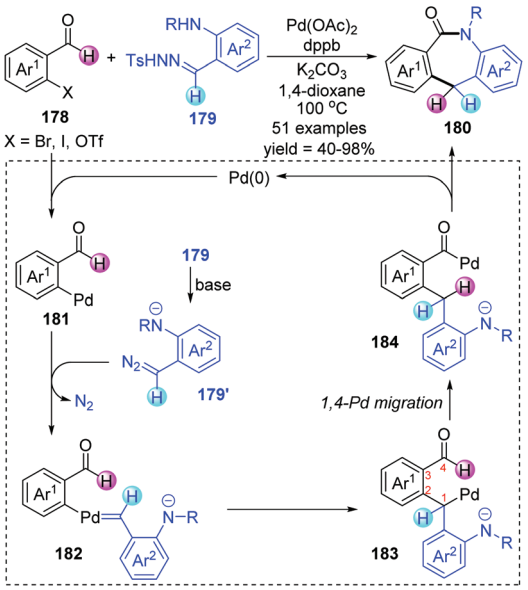

Scheme 31 Synthesis of dibenzo[*b*,*e*]azepin-6-one frameworks *via* two-component coupling.

(Scheme 31).[26] Broad substrate scope, excellent functional group tolerance, and feasible scale-up reactions gave this strategy practicality and synthetic potential. The transformation proceeded *via* an unconventional approach to functionalize the aldehyde C–H bond. A series of deuterium labelling experiments revealed the origin of hydrogen atoms on the central ring; a process of hydrogen atom migration from the acyl to the dibenzylic position should be involved in this conversion. Thus, a catalytic cycle involving 1,4-Pd migration was proposed as depicted. The initial oxidative addition between *o*-haloarylaldehydes **178** and a Pd(0) catalyst would generate Pd(II) intermediate **181**, which subsequently reacted with the *in situ* generated diazo compound **179′** to afford a palladium carbene intermediate **182**. Subsequent intramolecular metal carbene migratory insertion produced an alkyl palladium species **183**. The crucial alkyl-to-acyl 1,4-palladium migration occurred to give a benzoyl palladium complex **184**, which further underwent ring closure to furnish the target seven-membered N-heterocyclic products **180** and regenerate the Pd(0) catalyst.

2.4 1,5-Palladium migration

In 2004, Suffert and Bour described a new cyclization and C–H activation/Stille cross-coupling reaction of benzosuberone derivatives **185**, which was regioselective and controlled by stannylated reagents (Scheme 32).[27] In this study, a series of rearrangement products **189** were obtained in moderate yields by employing the vinylstannanes **188** as stannylated reagents. A 1,5-palladium migration was supposed to be responsible for this rearrangement; however, this migration process was totally suppressed and non-migratory product **187** was afforded when alkynylstannanes **186** were employed instead of **188**. Observation of deuterium labelling experiments strongly supported that a location swap between the Pd-group and aryl

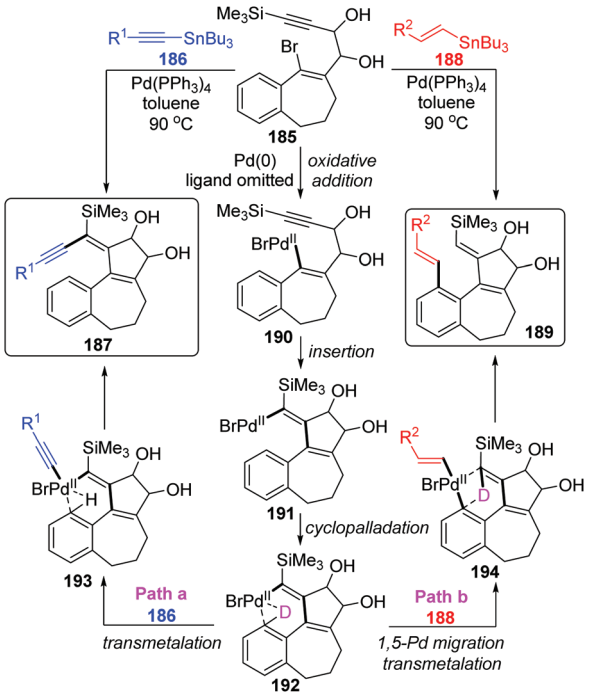

Scheme 32 Regioselective Stille cross-coupling reactions controlled by stannylated reagents.

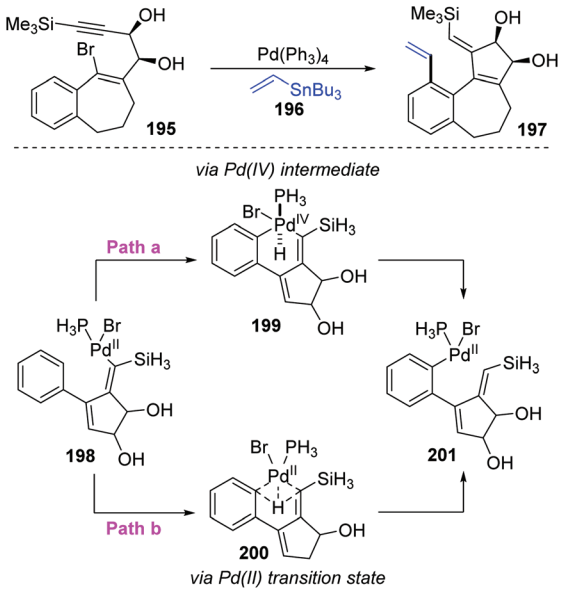

Scheme 33 1,5-Palladium migration involved cyclocarbopalladation-Stille coupling.

D atom occurred through the coordination sphere of palladium, as shown in compound **192**. A plausible mechanism is also illustrated in Scheme 32. Once the key intermediate **192** was generated *via* sequential oxidative addition of Pd(0) (**185** to **190**), insertion of a triple bond (**190** to **191**), and cyclopalladation *via* an agostic interaction (**191** to **192**), the transmetalation would take place directly between alkynylstannanes **186** and key intermediate **192** to furnish the non-migrated products **187** (path a). Alternatively, when vinylic reagents **188** were used instead (path b), the vinylic groups were preferentially installed on the aromatic position to provide rearrangement products **189** *via* 1,5-palladium shift from vinyl to aryl. The stereoelectronic factors of stannylated reagents were potentially related to such regioselectivity.

Later, the Dedieu group further carried out a DFT/B3LYP model study on this unusual 1,5 vinyl to aryl palladium shift that occurred in cyclocarbopalladation-Stille coupling tandem reaction (Scheme 33).[28] Two possible pathways were proposed for this migration. As shown in path a, a hydridophenylvinyl Pd(IV) intermediate **199** was formed *via* the phenyl C–H oxidative addition on the palladium atom, which subsequently underwent C–H reductive elimination to provide the phenyl Pd (II) complex **201**. Alternatively, in path b, a one-step process occurs, in which the bivalent oxidation state of the palladium atom is retained (species **200**). The energy computation of the various transition states and intermediates revealed that the possible mechanism of this migration preferred a one-step hydrogen transfer between the two negatively charged carbon atoms of the vinyl and phenyl groups (path b). The two-step pathway involving a Pd(IV) intermediate (path a) is not likely to take place.

In 2017, Nozaki and Shintani *et al.* developed a palladium/(*R*)-**L3**-catalyzed asymmetric synthesis of silicon-stereogenic 5,10-dihydrophenazasilines **203** (Scheme 34).[29] A series of mechanistic investigations were carried out, revealing that an enantioselective 1,5-palladium migration was involved in this conversion. And this migratory process also represented the first example of asymmetric induction at the step of metal migration itself. For this transformation, restriction of sub-

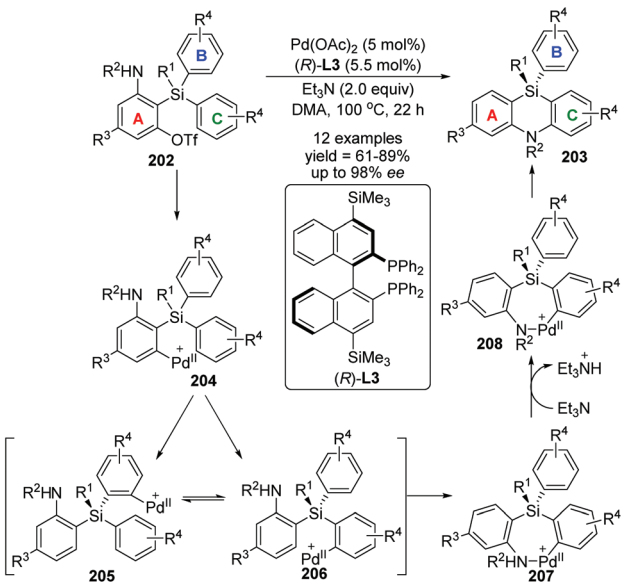

Scheme 34 Palladium-catalyzed asymmetric synthesis of 5,10-dihydrophenazasilines.

strates should be noticed, and functional group R^4 in the aromatic B and C must be kept in the same type and position, or a pair of isomers was obtained. The detailed catalytic mechanism is also shown in Scheme 34. The arylpalladium(II) compound **204** was generated *via* oxidative addition of **202** to Pd(0). Then, a 1,5-palladium migration occurred between two aryl groups to afford the Pd(II) species **205** or **206**, which was followed by intramolecular coordination of the amino group to the palladium center. The resulting compound **207** further turned into palladacycle **208** *via* Et_3N-assisted deprotonation. Final reductive elimination and C–N bond-forming provided the desired product **203** along with regeneration of the active Pd(0) catalyst. Moreover, a KIE (Kinetic Isotope Effect) investigation, KIE value = 1.31, revealed that the 1,5-palladium migration is not the turnover-limiting step for this transformation (Scheme 35).

Taking the 2-(dimethylphenylsilyl)phenyl triflates **211** as a model substrate, Nozaki and co-workers further theoretically examined the palladium-catalyzed reaction as shown in Scheme 36.[30] Computation pointed that the neutral diorganopalladium(II) intermediate **213** should be involved rather than a 1,5-palladium migration process when generating the dibenzosilole **214** (path a). On the other hand, in path b, a low-energy amine-coordinated palladacycle intermediate **216** should be present to drive the reaction toward 5,10-dihydrophenazasiline **218** instead of dibenzosilole **214**.

Early in this year, the Zhao group achieved an efficient remote C(sp^3)–H functionalization of a methyl group on silicon by employing three different types of nucleophiles, including carbene coupling, Suzuki coupling, and Miyaura borylation reaction (Scheme 37).[31] (8-Bromonaphthalen-1-yl) silane derivatives **219** could afford diverse vinyl (**220a**), benzyl (**220b**), and boryl silanes (**220c**) in moderate to excellent yields. This is the first example of a transformation involving 1,5-palladium migration from aryl to alkyl. The detailed catalytic cycle is illustrated in Scheme 38. Oxidative addition of **219** to Pd(0) could generate Pd(II) intermediate **224**, which underwent a successive σ-bond metathesis between the C(sp^2)–Pd bond and C(sp^3)–H bond (**225**) to form Pd-migrated species **226**. Alternatively, the formation of the Pd(IV)–H species **225′** *via* oxidative addition of the C(sp^3)–H bond to Pd(II) intermediate **224** and subsequent reductive elimination could also be responsible for **226**. In path a, the reaction of intermediate **226** with the carbene precursor generated from **221** could give a Pd(II)-carbene complex **227**. The following migratory insertion afforded the C(sp^3)–Pd(II) species **228**, and further β-hydride elimination delivered vinylsilane product **220a** and regenerated the Pd(0) catalyst. In path b, transmetalation between Pd(II) intermediate **226** and aryl boronic acid (or B_2pin_2) led to either the Pd(II) species **229** or **230**. Final reductive elimination resulted in the corresponding products and released Pd(0).

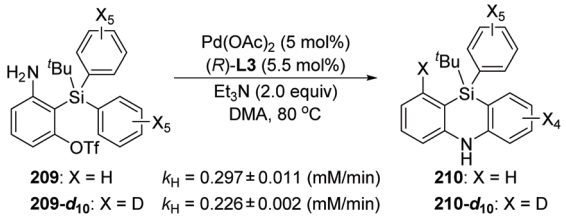

Scheme 35 Kinetic isotope effect investigations during 1,5-palladium migration.

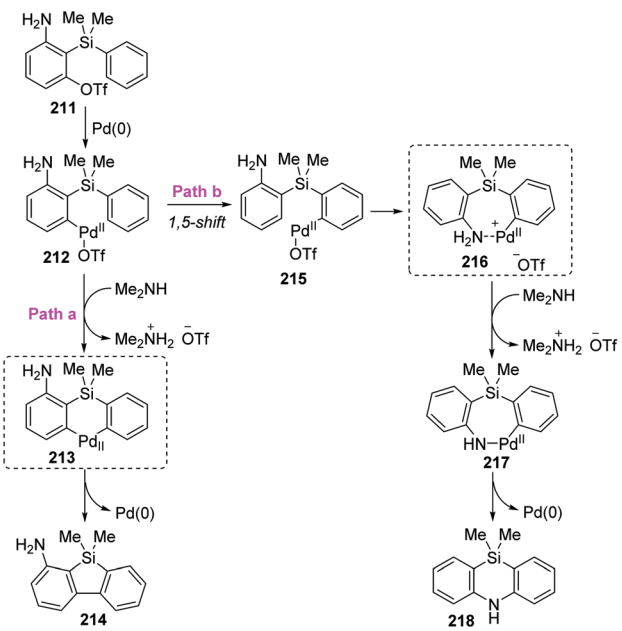

Scheme 36 Proposed catalytic cycle for the conversion of **211** to **218**.

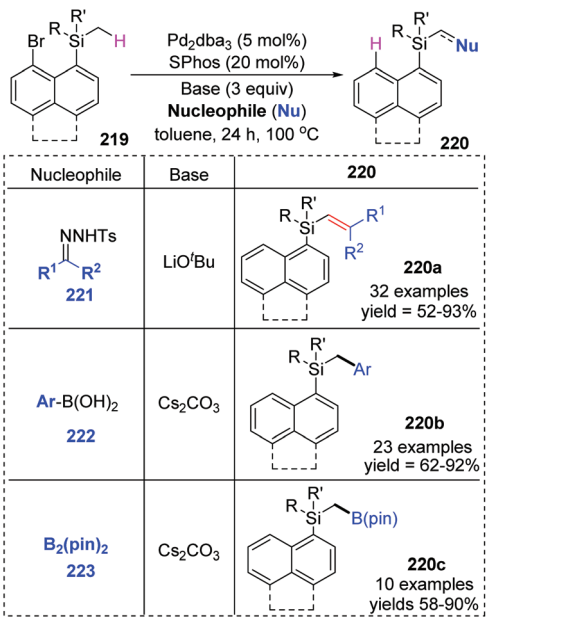

Scheme 37 Palladium-catalyzed remote C(sp^3)–H functionalization of the methyl group on silicon.

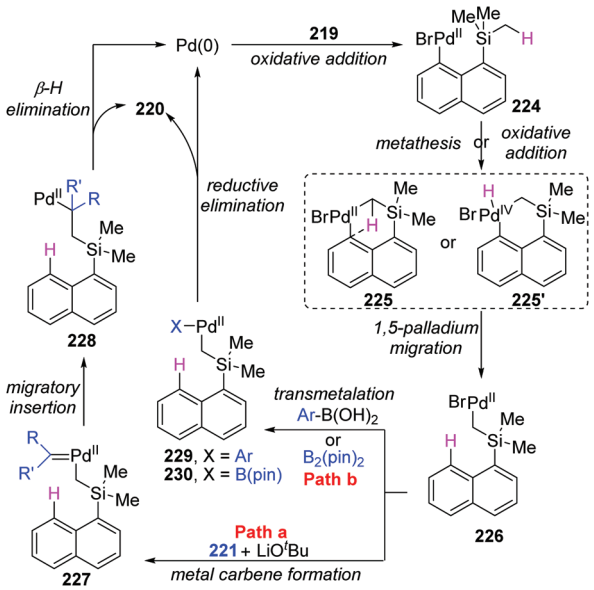

Scheme 38 Proposed mechanism for the C(sp^3)–H functionalization of the methyl group on silicon.

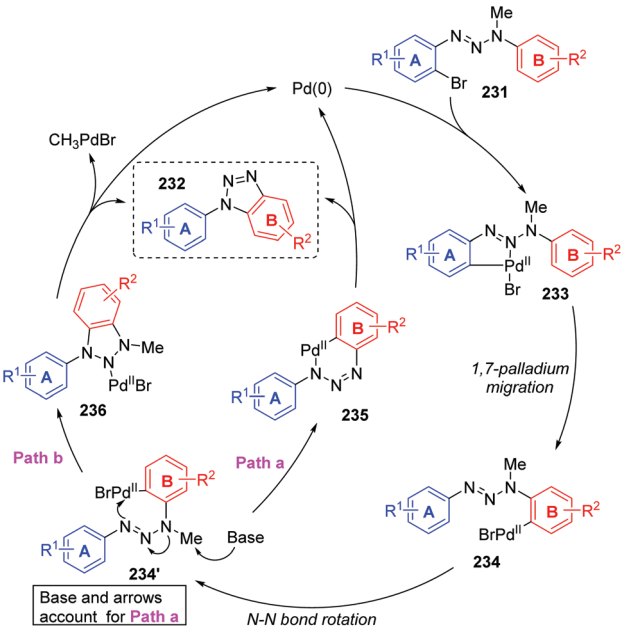

Scheme 40 Proposed mechanism for the synthesis of benzotriazoles.

2.5 1,7-Palladium migration

In 2011, Ren and co-workers reported a novel strategy for the regioselective synthesis of benzotriazoles **232** *via* a sequential 1,7-palladium shift/cyclization/dealkylation process (Scheme 39).[32] The transformation was performed at 110 °C or 150 °C to give the target products in excellent yields with high regioselectivity. A possible reaction mechanism for this transformation is depicted in Scheme 40. Initially, oxidative addition of Pd(0) to a C(sp^2)–Br bond generated the intermediate **233**. Then, the coordination of palladium with the middle nitrogen atom of the triazene moiety would make it close enough to the other aromatic ring, which allowed the 1,7-Pd migration to take place *via* C–H bond activation to give species **234** (an eight-membered-ring palladacycle intermediate[33] might be involved). With the aid of a base, compound **234′** suffered intramolecular cyclization to afford the six-membered-ring palladacycle intermediate **235** (path a), which would provide the final product **232** and release the Pd(0) catalyst. An alternative reaction pathway (path b) cannot be excluded; **234′** could form a five-membered ring **236** by the insertion of an N=N double bond into a C–Pd bond, and the final β-CH_3 elimination would also be possible to furnish the target product **232**.

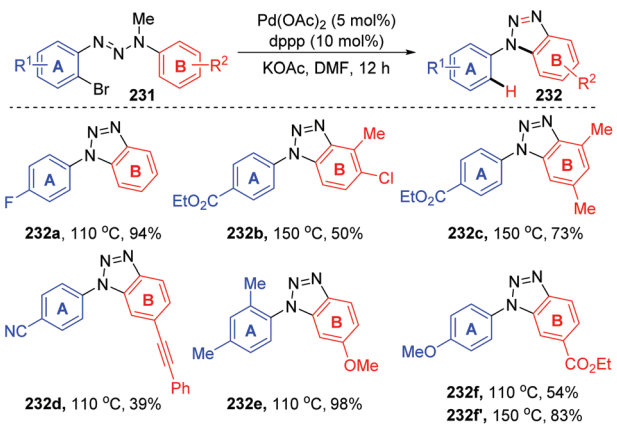

Scheme 39 Pd-Catalyzed intramolecular amination for the synthesis of benzotriazoles.

2.6 Other types of palladium migration

In 2002, Larock and co-workers reported a novel long-chain palladium migration strategy involving three-component coupling of 3-iodopyridine, long-chain nonconjugated dienes and appropriate nitrogen nucleophiles (Scheme 41).[34] This transformation provided a convenient approach to prepare the pyridine alkaloids and related natural products, which contained a long chain with an aromatic or heteroaryl group on one end of

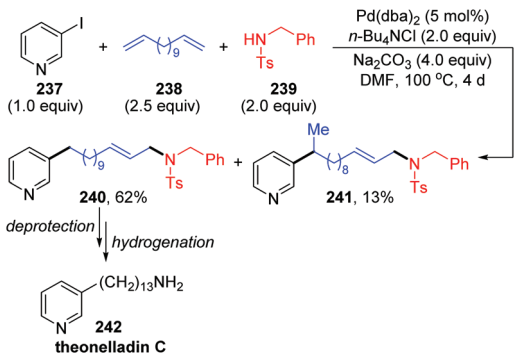

Scheme 41 Three-component coupling reaction *via* palladium long-distance migration.

the chain and diverse functional groups on the other end. For example, as shown in Scheme 41, employing 1,12-tridecadiene **238** as the long-chain dienes, followed by deprotection and hydrogenation, would afford the natural product theonelladin C **242** readily. However, there are still some shortcomings in this reaction. Ammonia and primary amines did not work well in this three-component coupling process. And the by-product isomer **241**, generated *via* introducing a pyridylpalladium group to the more hindered internal carbon was inevitable.

3 Rhodium migration

3.1 1,3-Rhodium migration

In 2013, the rearrangement of Rh(I) 2,6-dimethoxybenzoate complex **243** *via* an unusual 1,3-Rh migration process was reported by the Zhao and Sun group (Scheme 42).[35] 2,4-Dimethoxybenzoate **244** was obtained in 71% yield under a CO_2 atmosphere while only 34% yield was obtained under a N_2 atmosphere, indicating that a decarboxylation/carboxylation process should be involved in this transformation. Decarboxylation of **243** generated a Rh(I) 2,6-dimethoxyphenyl intermediate **245**, which then underwent 1,3-Rh/H shift to form the migrated Rh(I) 2,4-dimethoxybenzoate species **246** with reduced steric strain. Final reinsertion of CO_2 into the Rh-aryl bond gave the more stable complex **244**. This 1,3-Rh migration also took place in analogical transformation. For example, 2,6-dimethoxybenzoic acid **247** reacted with *t*-butyl acrylate **248** smoothly under a trace of rhodium catalyst to provide migrated product **250** in good yield and selectivity. A proposed pathway for this 1,3-Rh migration is illustrated in Scheme 43. A deuterium-labeling study revealed that two consecutive 1,4-migrations mediated by a methoxy group should be responsible for the resulting 1,3-Rh migration. The starting cyclometalation of aryl-Rh(I) **251** activated the Csp^3–H bond of methoxy at the *ortho* position and generated a Rh(III) hydrido intermediate **252**, followed by reductive elimination to afford a Rh(I) aryloxyalkyl **253**. Further activation of the aromatic C–H bond at the less hindered *meta* position afforded another Rh(III) cyclometalated species **254**, which underwent reductive elimination at the methoxy position to produce the final product **255**.

In 2015, synthesis of stereochemically complex azabicyclic structures *via* Rh(III)-catalyzed allylic $C(sp^3)$–H activation/electrocyclization was achieved by Rovis and Archambeau (Scheme 44).[36] Unsaturated *N*-tosylsulfonamide **256** reacted with diphenylacetylene **257** to afford the desired products **258** with complete control of diastereoselectivity, and the phenyl

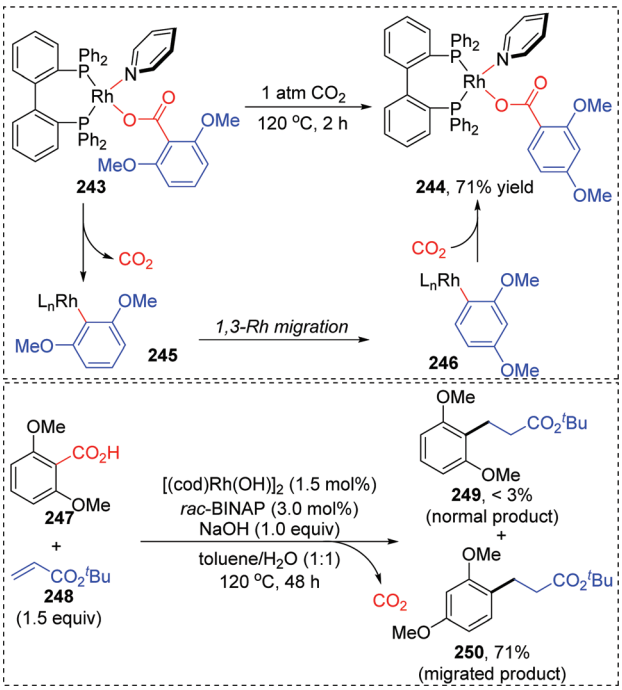

Scheme 42 Rearrangement of Rh(I) 2,6-dimethoxybenzoate derivatives *via* 1,3-Rh migration.

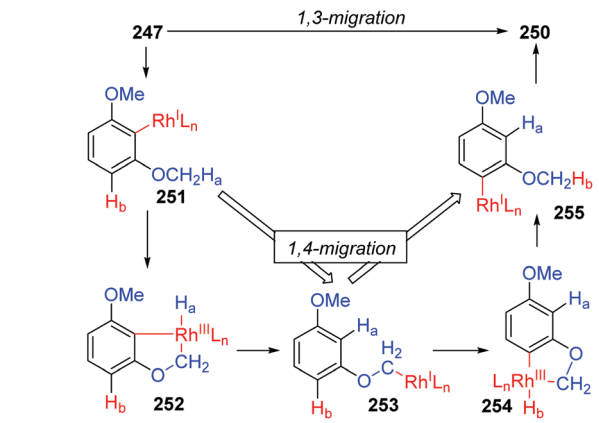

Scheme 43 Proposed mechanism for 1,3-Rh migration in the rearrangement of the Rh(I) complex.

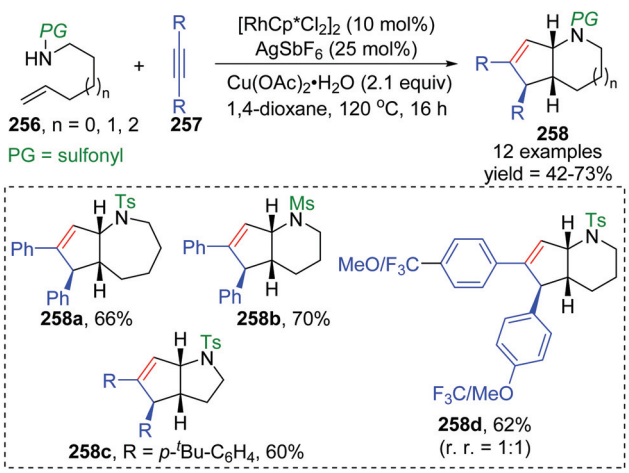

Scheme 44 Rh-Catalyzed synthesis of azabicyclic derivatives from unsaturated *N*-sulfonamides.

group was located on the *exo*-face of the molecule. Rh(III), Ag(I) and Cu(II) species, and high reaction temperature (120 °C) were all necessary for this conversion, while the reaction was shut down when the temperature decreased to 80 °C. Moreover, substituents on both sides of alkyne **257** should stay the same because the electronic properties of the alkyne did not influence the regioselectivity; for instance, an unsymmetrical alkyne led to a mixture of products **258d**. The results of deuterium-labeling experiments strongly supported a 1,3-Rh migration process involved in the catalytic cycle as illustrated in Scheme 45. Initially, the allylic C(sp^3)–H bond of **259** was activated by a Rh(III) catalyst, generating a π-allyl complex **260** and the homologous isomer **261**. Subsequent migratory insertion of alkyne **262** to **261** led to the vinylrhodium(III) species **263**, which underwent vinyl-to-allyl 1,3-Rh migration to afford the bis(allyl)rhodium(III) complex **264**. Affected by steric resistance, the following 4π-electrocyclization preferred to form a π-allylrhodium(III) **266** with specific stereo-configuration. Successive *N*-metalation and reductive elimination gave the target dicyclo-product **268** and Rh(I) species. Final copper-mediated oxidation of the resulting Rh(I) species regenerated the active Rh(III) catalyst.

3.2 1,4-Rhodium migration

Among various types of metal-migration involved reactions, 1,4-rhodium migration is another well-studied subject no less than 1,4-palladium migration during the past twenty years. This chapter only summarizes several new reports published recently, and more information toward 1,4-rhodium migration can be found in Gu's review.[4]

The Tian and Dou group achieved a rhodium-catalyzed expeditious synthesis of indenes **270** from propargyl alcohols **269** and arylboronic acids *via* the selective 1,4-rhodium migration over β-oxygen elimination (Scheme 46).[37] Ligands

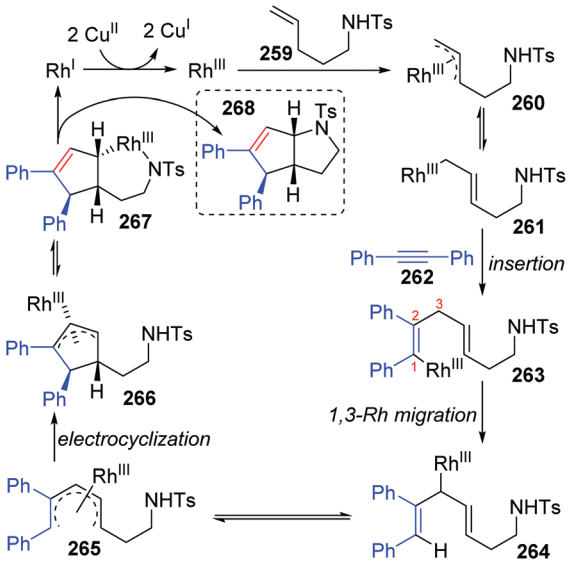

Scheme 45 Proposed mechanism for the synthesis of azabicyclic derivatives.

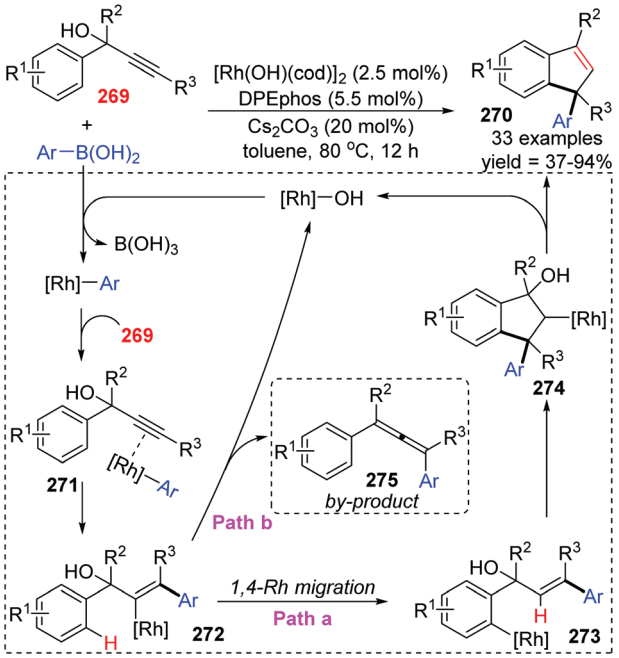

Scheme 46 Rhodium-catalyzed synthesis of indenes from propargyl alcohols and organoboronic acids.

played a crucial role in this transformation, and DPEphos was found to be uniquely effective for the high selectivity of migratory products. Results of density functional theory (DFT) calculations revealed that the employment of DPEPhos as the ligand lowered the relative energy toward key intermediates of the 1,4-migration path. As illustrated in Scheme 46, a plausible mechanism involving 1,4-Rh shift is responsible for the indene products. Initially, an arylrhodium intermediate was generated *via* transmetalation of the hydroxorhodium catalyst with arylboronic acids, which further coordinated with alkynyl to afford the vinylrhodium complex **272** by regioselective *syn*-arylrhodation. In path a, 1,4-rhodium migration from **272** gave an arylrhodium species **273**, followed by a second intramolecular arylrhodation to form the key alkylrhodium intermediate **274**. Ultimately β-oxygen elimination occurred to furnish the target indene derivatives **270** and regenerated the active Rh catalyst simultaneously. Alternatively, premature β-oxygen elimination of intermediate **272** would lead to the allene products **275** (path b).

Lam and co-workers developed a rhodium-catalyzed arylative cyclization of alkynyl malonates **276** with arylboronic acids *via* 1,4-rhodium(I) migration to prepare functionalized 1-tetralones **277** in good yields (Scheme 47).[38] This strategy performed excellently by using KF as a base in 1,4-dioxane/H_2O (9 : 1) as the solvent. And additionally, the stereo-configuration of the products could be affected by the chirality of the ligands. Preliminary synthesis of chiral products (+)-**281** (76% ee) along with an inseparable mixture of **282** and **283** was achieved by employing a chiral bisphosphine-rhodium complex as the precatalyst; however, no further investigation toward enantioselectivity has been conducted. Although the

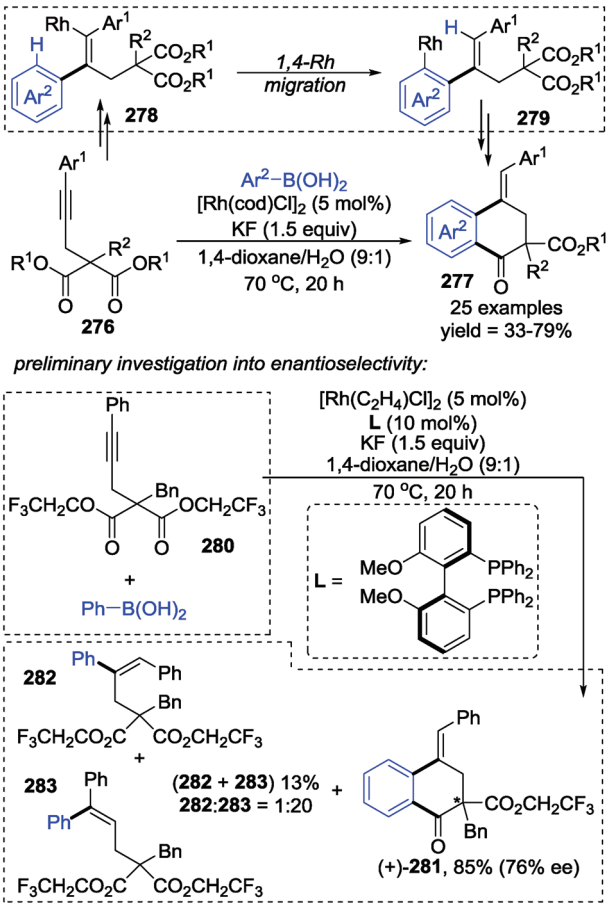

Scheme 47 Rh-Catalyzed arylative cyclization of alkynyl malonates with arylboronic acids.

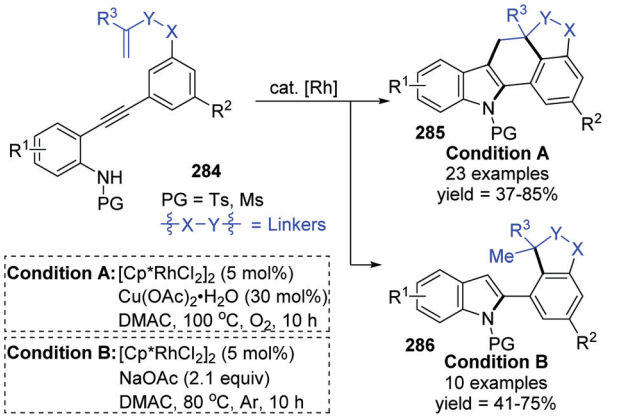

Scheme 48 Rh(III)-Catalyzed reaction to prepare diversified indole-fused polycycles.

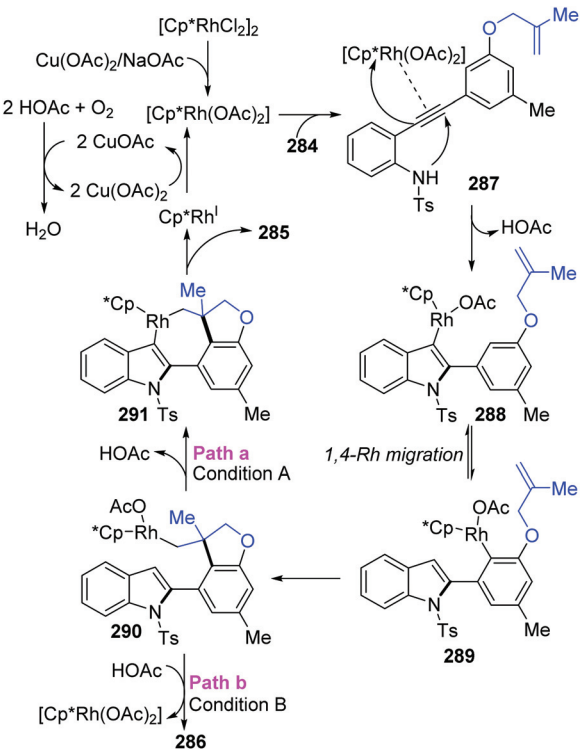

Scheme 49 Proposed catalytic pathway for the synthesis of indole-fused polycycles.

reaction mechanism was not proposed, an alkenyl-to-aryl 1,4-Rh(I) migration was considered to be the key step for the generation of a benzo six-membered heterocycle, as shown from **278** to **279**.

The Lin and Yao group reported a rhodium(III)-catalyzed strategy for the divergent construction of indole-fused polycyclic frameworks *via* an aryl-to-aryl 1,4-Rh migration process (Scheme 48).[39] Different types of products were obtained by changing the reaction conditions. Carboannulation product **285** was afforded in the presence of Rh and $Cu(OAc)_2 \cdot H_2O$ catalysts under an oxygen atmosphere, while hydroarylation product **286** was generated by employing a Rh catalyst and NaOAc under an argon atmosphere. A plausible pathway is illustrated in Scheme 49. Initial coordination of active Rh(III) to alkynyl and subsequent intramolecular electrophilic cyclization furnished the 3-indolyl rhodium species **288**. Subsequently, C–H bond activation/aryl-to-aryl 1,4-rhodium migration took place to generate an aryl rhodium intermediate **289**, which underwent intramolecular migratory insertion of the alkene to the Rh–C bond to give the alkyl rhodium intermediate **290**. In path a (condition A), the indole C3 C–H activation offered the seven-membered rhodacycle complex **291**. Final reductive elimination provided the target pentacyclic product **285**, and the active Rh(III) catalyst was regenerated from Rh(I) *via* oxidation with the assistance of $Cu(OAc)_2/O_2$. Alternatively, in path b (condition B), the alkyl rhodium intermediate **290** underwent a direct protonation/demetalation process to afford 2-aryl indoles **286** and regenerate the Rh(III) catalyst.

A chiral bisphosphine–rhodium complex promoted diastereo- and enantioselective reaction of arylboronic acids **293** with alkynyl 1,3-diketones was achieved by Lam and coworkers (Scheme 50).[40] Both acyclic and cyclic 1,3-diketones

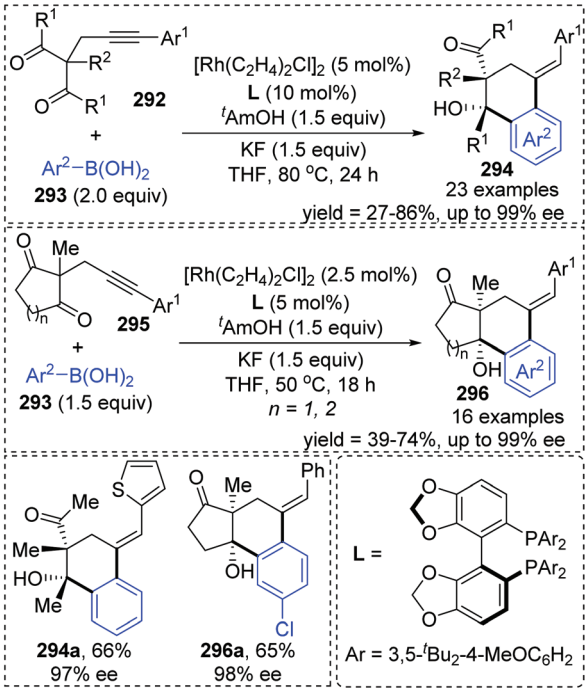

Scheme 50 Rhodium/chiral-bisphosphine complex catalyzed reaction of arylboronic acids with alkynyl 1,3-diketones.

(**292** and **295**) performed effectively to afford the corresponding arylative cyclization product **294** and **296** with high enantioselectivity in moderate to good yields. An alkenyl-to-aryl 1,4-Rh(I) migration process played a significant role in this transformation (Scheme 51). Initially, a chiral complex **297** consisting of one bisphosphine bound to one rhodium atom was formed from the mixture of $[Rh(C_2H_4)Cl]_2$, **L**, KF, and *t*-AmOH, which further turned into an arylrhodium species **299** *via* transmetalation with $PhB(OH)_2$. Taking **300** as an example, the successive migratory insertion and 1,4-rhodium shift provided the key arylrhodium intermediate **302**. The relative configuration of products **294** could be explained by an experimental stereochemical model where cyclization proceeds through a conformation similar to intermediate **303**. Specific coordination of one ketone to the rhodium atom enabled the carbonyl group to be aligned with the arylrhodium bond, and the second ketone was coordinated to rhodium in an axial position. Depending on the geometric constraints, subsequent nucleophilic attack and migratory insertion formed the resulting configuration **304**, which underwent protonation to afford target products **294**.

Matsuda and co-workers achieved a rhodium(I)-catalyzed addition of arylboronic acids **306** to β-(arylethynyl) ketones **305**, involving an aryl-to-aryl 1,4-rhodium migration process (Scheme 52).[41] The conversion started with the regioselective addition of an arylrhodium(I) species to the alkyne moiety of ketone **308**, followed by 1,4-rhodium migration generating an arylrhodium(I) species **309**. Intramolecular nucleophilic addition and subsequent protonation were responsible for the formation of the six-membered ring. The resulting tetralin alcohols **310** further underwent dehydration/aromatization upon treatment with Tf_2O, providing access to various fused aromatic compounds **307**.

3.3 1,5-Rhodium migration

In 2018, a Rh(III)-catalyzed annulation of 2-alkenyl anilides **311** with alkynes **312** *via* C–H activation was developed by the Mascareñas and Gulías group, providing a series of 2-substituted indoline derivatives **313** (Scheme 53).[42] Various alkyne

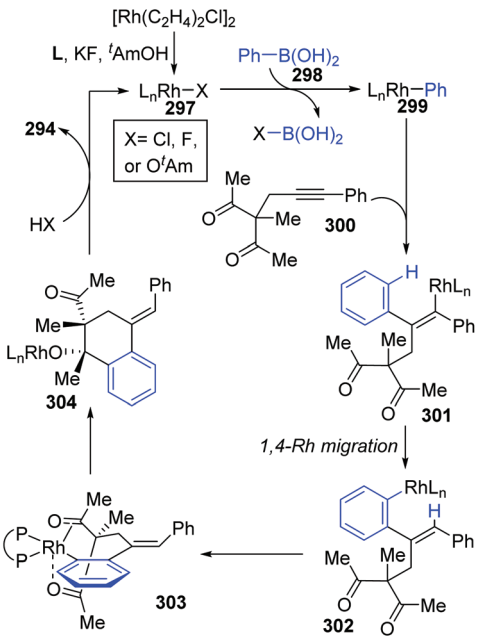

Scheme 51 Proposed catalytic mechanism for the reaction of arylboronic acids with alkynyl 1,3-diketones.

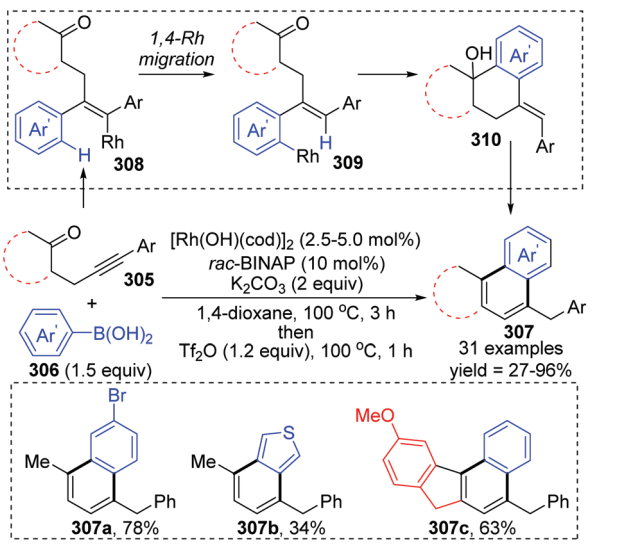

Scheme 52 Rhodium(I)-catalyzed reaction of β-(arylethynyl)ketones with boronic acids.

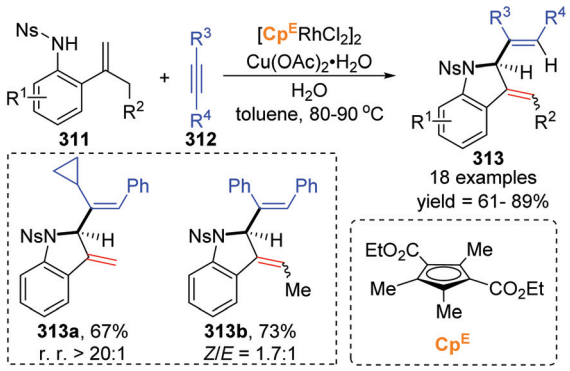

Scheme 53 Rhodium(III)-catalyzed annulation of 2-alkenyl anilides with alkynes.

components were well tolerated, and symmetrical alkynes with electron-rich or deficient aromatic substituents performed smoothly to give the corresponding products in good yields. Additionally, high regioselectivity was observed when nonsymmetrical alkynes were employed, favoring products with the aryl substituent at the terminal position of the alkene, such as **313a** (rr > 20 : 1). According to deuterium scrambling investigations, the possible reaction pathway is illustrated in Scheme 54. An active rhodium acetate species **314** was formed, which underwent ligand exchange of one of the acetates with the amide of **311** to generate a complex **315**. Thereafter, activation of the alkenyl C–H bond and carbometalation took place to afford a rhodacycle **316**, followed by migratory insertion of the 1,2-diphenylethyne to give a new rhodacycle intermediate **317**. Successive internal 1,5-hydrogen/rhodium exchange and reductive elimination afforded the corresponding indoline product **313**. Active Rh catalyst was regenerated with the assistance of $Cu(OAc)_2$.

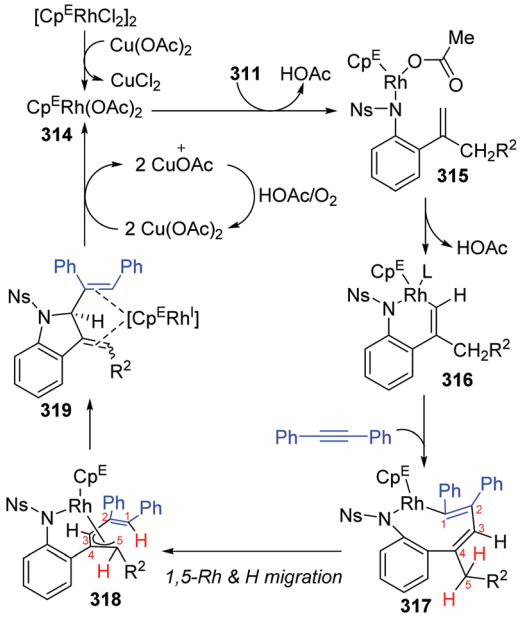

Scheme 54 Possible mechanism for the cyclization of 2-alkenyl anilides.

4 Iron migration

4.1 1,4-Iron migration

Formal iron migration reports emerged in 2018, Ackermann and co-workers described a strategy toward iron-catalyzed C–H/N–H/C–O/C–H activation and functionalization assisted by removable triazoles (Scheme 55).[43] A variety of methylene-tethered triazoles **320** was converted into the corresponding isoquinolones **322** at room temperature, and further synthesis of nonaromatic *exo*-methylene dihydroisoquinolines **325** was also achieved by replacing the THA group with a dimethylmethylene TAM group. Various functional groups were tolerated in this transformation, for example, bromo substituents on arenes survived very well to provide target product **322a** in high yields. Based on the results of preliminary mechanism investigations, a possible reaction pathway involving a formal 1,4-iron migration process is demonstrated in Scheme 56. Taking substrate **326** as an example, initial facile C–H metalation generated an aryliron complex **327**, followed by allene migratory insertion to afford the intermediate **329**. Then oxidation-induced reductive elimination of **329** formed an allyl iron species **330**, which experienced 1,4-iron migration to give the stabilized allylic-benzylic iron intermediate **331**. The process of 1,4-iron/hydrogen shift was strongly supported by deuterium-labeling experiments. Ultimate proto-demetalation with the amide motif of the substrate **331** furnished *exo*-methylene-3,4-dihydroisoquinoline **332**, and further isomerization generated the corresponding isoquinolone products **322**.

An iron-catalyzed *ortho*-selective C–H alkylation of aromatic ketones **334** with *N*-alkenylindoles **333** by employing a

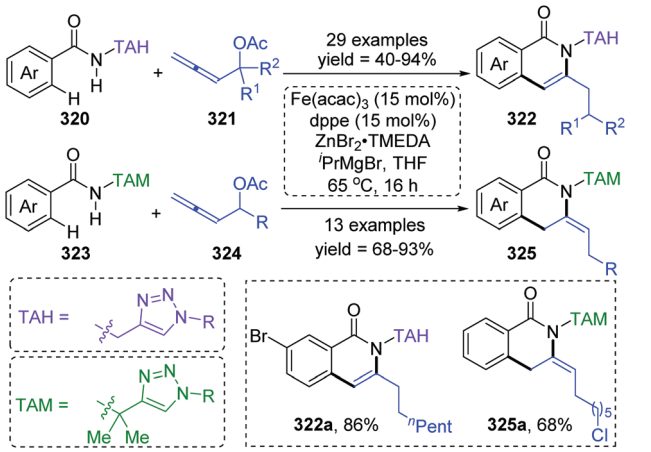

Scheme 55 Ackermann's strategy of Fe-catalyzed C–H/N–H/C–O/C–H activation.

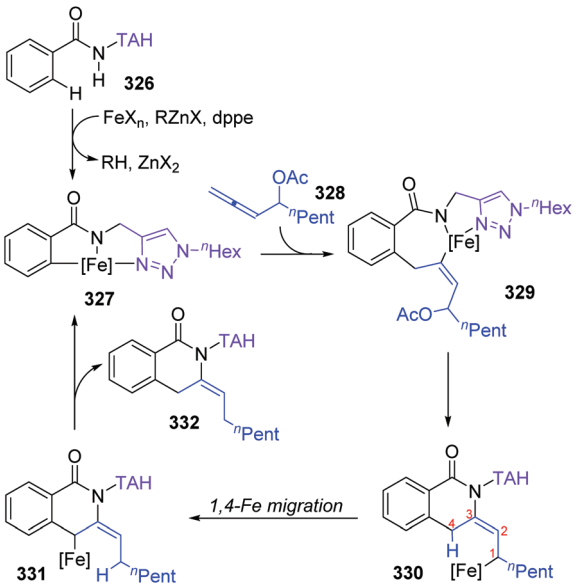

Scheme 56 Possible reaction mechanism for the synthesis of isoquinolones and dihydroisoquinolines.

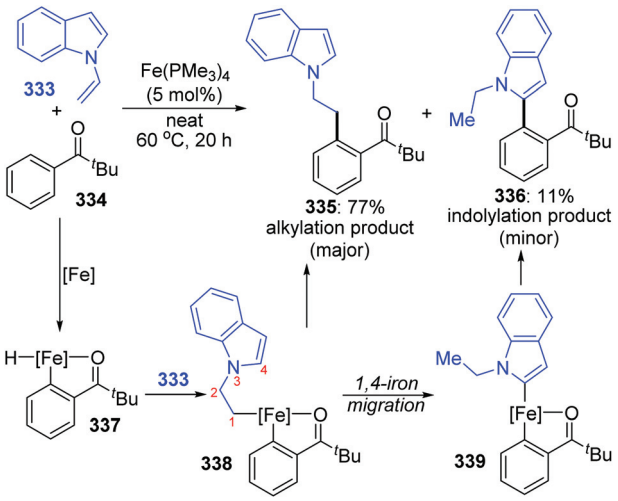

Scheme 57 Iron-catalyzed *ortho*-selective C–H alkylation of aromatic ketones with *N*-alkenylindoles.

$Fe(OMe_3)_4$ catalyst was developed by Kakiuchi and co-workers (Scheme 57).[44] A minor product indolylation species **336** was considered to occur *via* a 1,4-iron migration procedure. As shown, initial C–H oxidative addition of aromatic ketones **334** to the iron catalyst and subsequent hydrometalation of *N*-alkenylindoles **333** gave an organoiron complex **338**. The uncommon alkyl-to-aryl 1,4-iron migration prior to reductive elimination took place to form an indolyliron intermediate **339**, which was responsible for the minor indolylation product. Although the indolylation product **336** was obtained in very low yield, it offered a new perspective for direct introduction of an aryl group at the *ortho* position of aromatic ketones.

4.2 1,5-Iron migration

A novel 1,5-iron migration was observed in Fe-catalyzed arylation of the aliphatic C–H bonds of 2-iodoalkylarenes **340** by Nakamura and Ilies *et al.* (Scheme 58).[45] Long alkyl chains were arylated with high regioselectivity at the γ-C–H bond by employing an iron(III) salt and a N-heterocyclic carbene ligand, providing diverse arylated alkanes **341** whose synthesis typically relied on transition-metal-catalyzed cross-coupling using alkyl halides that were difficult to access. Proposed key reaction intermediates are illustrated in Scheme 59. An organoiron complex Ph-[Fe] was envisioned to be generated from the iron salt and organometallic reagent, which might add to the aryl iodide **340** *via* single electron transfer (SET) to generate an iron intermediate **344**. Notably, unlike the classical type of metal migration discussed above, this iron migration was supposed to occur *via* a radical pathway. The preliminary suggestion was that **344** behaved in a radical manner and cleaved the aliphatic C–H bond *via* 1,5-hydrogen/iron shift to afford an alkyliron species **345**, which then furnished the target product **342** through reductive elimination. However, no direct evidence supports this conclusion yet, and further investigations are imperative. Moreover, the reaction quenched with D_2O

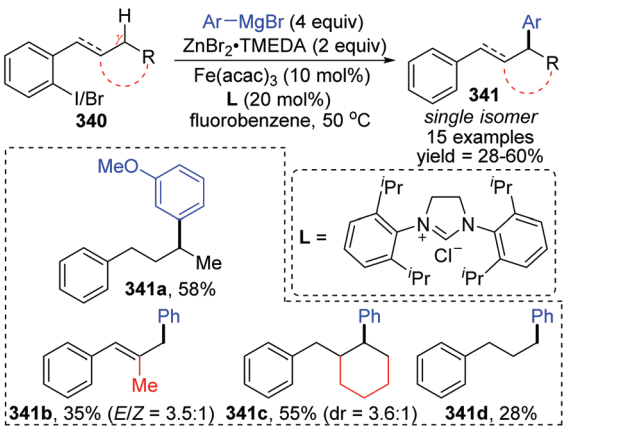

Scheme 58 Iron-catalyzed remote arylation of aliphatic C–H *via* a 1,5-Fe shift.

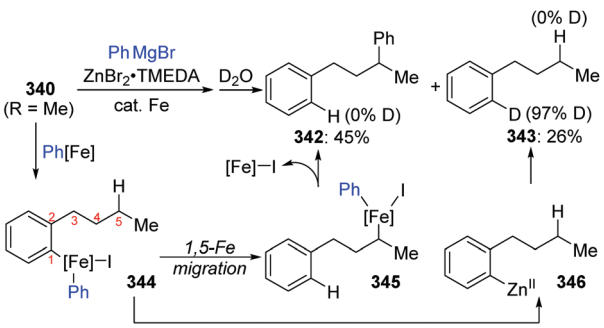

Scheme 59 Deuterium labeling experiment for Fe-catalyzed remote arylation.

afforded the phenylated product **342** with no deuterium incorporation, while the dehalogenated by-product **343** exhibited 97% deuterium incorporation on the carbon where the iodine atom was located. The existence of by-product **343** also should be responsible for the relatively low conversion yields.

5 Cobalt migration

Until now, all three reports involving cobalt migration have come from Yoshikai's team. In 2012, the first example of cobalt-migration involving reactions was described by Yoshikai and co-workers.[46] Diverse *ortho*-alkenylarylzinc species **349** were prepared by addition of arylzinc reagents **347** to alkynes **348** in the presence of Co-catalyst (Scheme 60). In the beginning, arylcobalt species were generated from the arylzinc reagents and active Co-catalyst, and the subsequent insertion into the alkyne formed an alkenylcobalt intermediate **351**. Then, 1,4-cobalt migration *via* C–H bond activation took place to afford an *ortho*-alkenylarylcobalt species **352**, which underwent transmetalation with the arylzinc reagent **347** to furnish a crucial *ortho*-alkenylarylzinc species **349** and regenerate the arylcobalt species. By employing different external electrophiles, the *ortho*-alkenylarylzinc species **349** could be easily converted into various corresponding products efficiently.

In the next four years, the Yoshikai group further developed two strategies involving 1,4-cobalt migration by using arylzinc reagents: (i) synthesis of *o*-(2-*exo*-norbornyl)arylzinc species **353** *via* addition of arylzinc reagents to norbornene derivatives **354** (Scheme 61),[47] and (ii) cyclization of acetylenic esters/ketones **360** with arylzinc reagents (Scheme 62).[48] As shown in Scheme 61, the transformations of preparing *o*-(2-*exo*-norbornyl)arylzinc compounds **355** proceeded in a similar way as the first example described above; however, an alkyl-to-aryl 1,4-coblat migration occurred instead of the vinyl-to-aryl one. Then, common electrophilic trapping reactions under copper or palladium catalysis gave diverse products in excellent yields, such as **356b** and **356c**. The third case illustrated in Scheme 62 is slightly different from the first two cases; without extra electrophiles, a diarylzinc reagent was utilized to react with acetylenic esters/ketones **360** to prepare a series of benzo-fused cyclic ketone or alcohol products (**361** and **362**). Likewise, starting with the formation of arylcobalt species, successive insertion of alkynes and vinyl-to-aryl 1,4-coblat migration took place to

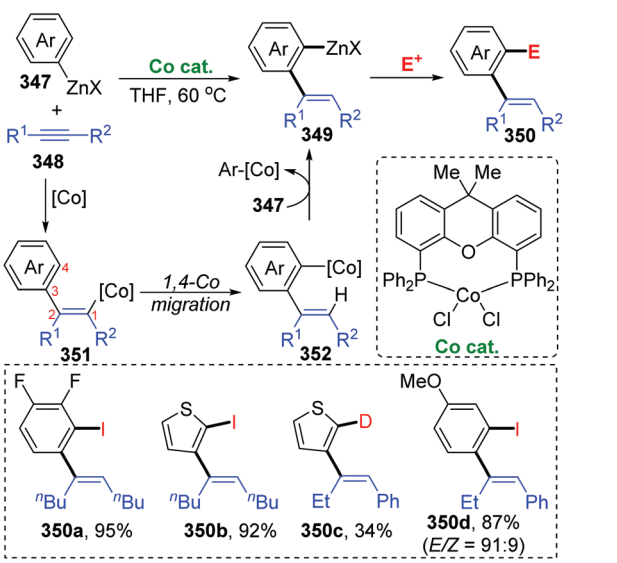

Scheme 60 Yoshikai's cobalt-catalyzed addition of arylzinc reagents to alkynes.

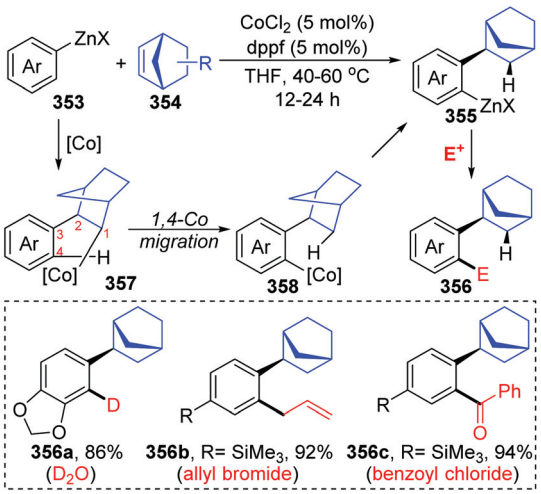

Scheme 61 Co-Catalyzed synthesis of *o*-(2-*exo*-norbornyl)arylzinc species from arylzinc reagents.

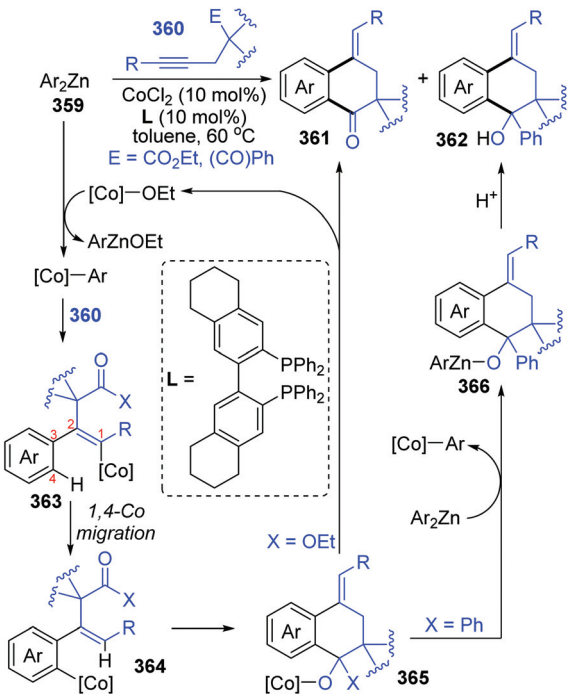

Scheme 62 Co-Catalyzed cyclization of acetylenic esters/ketones with arylzinc reagents.

form an *ortho*-alkenylarylcobalt complex **364**. In the presence of an intramolecular carbonyl group, 6-*exo*-cyclization occurred readily to afford bicyclic skeleton intermediate **365**. Subsequent β-alkoxy elimination furnished the benzo-fused cyclic ketones **361** (X = OEt) with a concomitant Co–OEt species, which further underwent transmetalation with the arylzinc reagent to regenerate the arylcobalt species. Alternatively, direct transmetalation of **365** with the arylzinc reagent could give a zinc alkoxide compound **366** and regenerate the arylcobalt species straight (X = Ph). The benzo-fused cyclic alcohol products **362** were obtained *via* protonation of zinc alkoxide compound **366**.

6 Iridium migration

In 2014, a iridium-catalyzed three-component coupling reaction of 1,3-enynes with arylboronic acids and triazinanes was achieved by Lam and co-workers *via* alkenyl-to-allyl 1,4-iridium (I) migration, furnishing diverse 1,5-functionalized 1,3-dienes **370** (Scheme 63).[49] The conversion started with transmetalation of an active iridium complex with arylboronic acid, which generated an aryliridium species. Further coordination and insertion of alkyne into the aryliridium species led to the alkenyliridium intermediate **371**, which subsequently turned into an allyliridium species **372** *via* alkenyl-to-allyl 1,4-iridium(I) migration. Then, the complex **373** was formed as a result of an σ–π–σ isomerization of species **372**. Subsequent allylation of imine **374** with complex **373** through a chair-like conformation **376** (major transition state) afforded the iridium amide **377**, which offered the final product **370** by protonation. Alternatively, the formation of conformation **375** (minor transition state) was responsible for the *E*/*Z* isomers of the target products.

Later the same year, Lam *et al.* reported another case involving 1,4-iridium migration. Various complex polycycles **380** were prepared with good stereoselectivity *via* iridium-catalyzed arylative cyclization of alkynones **378** (Scheme 64).[50] The transformation of **378** was conducted with $PhB(OH)_2$ in the presence of $[\{Ir(cod)Cl\}_2]$ (1.5 mol%), KF (1.5 equiv.) as a mild base, and *t*-BuOH (1.5 equiv.) as a proton source. After the formation of [Ir]-O*t*-Bu from a precatalyst, an aryliridium species was formed subsequently *via* transmetalation between the [Ir]-O*t*-Bu and arylboronic acid. Migratory insertion of the alkyne **378** to aryliridium species took place to afford alkenyliridium complex **381**, and then an alkenyl-to-aryl 1,4-iridium migration occurred to give the aryliridium intermediate **382**. In the presence of an intramolecular carbonyl, the 6-*exo* cyclization triggered by nucleophilic attack generated a tertiary-alcohol-containing tricycle **383**, followed by protonation to furnish the final product **380** and concomitant iridium butoxide.

The appearance of iridium-migration was also observed in the reaction of phenyliridium(III) complex [Cp*IrCl-(Ph)(PMe_3)] **384** with PhC≡CMe in the presence of $NaBAr^F_4$ at 25 °C, which furnished a π-allyl complex **388** as the end product in 86% yield (Scheme 65).[51] Ishii and co-workers studied the intermediates of the reaction in depth by single-crystal X-ray and deuterium labeling experiments, and pointed out that both 1,3- and 1,4-iridium migration was involved in the formation of π-allyl complex **388**. The procedure is also depicted in Scheme 65. This π-allyl complex **388** was produced *via* two distinct mechanisms, (i) C=C bond rotation in **385** and subsequent direct vinyl-to-allyl 1,3-Ir migration (path a), and (ii) successive vinyl-to-aryl and aryl-to-allyl 1,4-Ir migrations (path b).

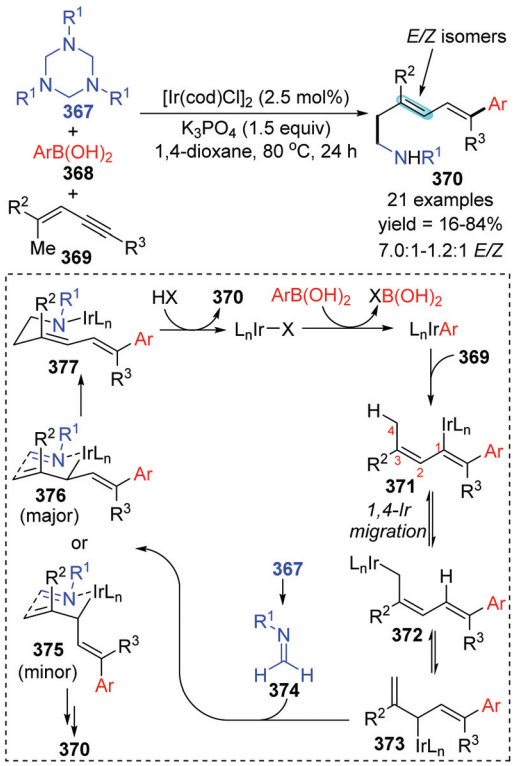

Scheme 63 Ir-Catalyzed 1,5-difunctionalization of 1,3-enynes with arylboronic acids and triazinanes.

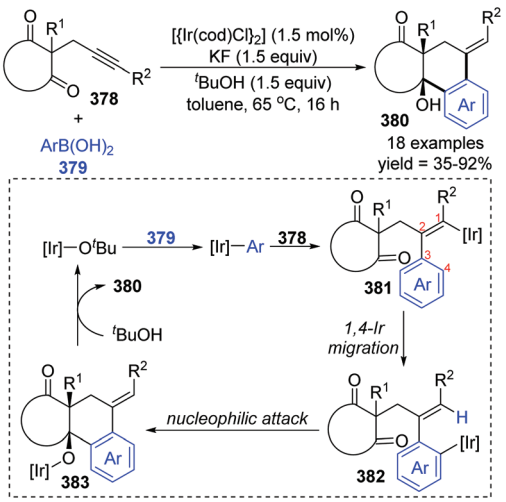

Scheme 64 Lam's strategy toward the iridium-catalyzed cyclization of alkynones.

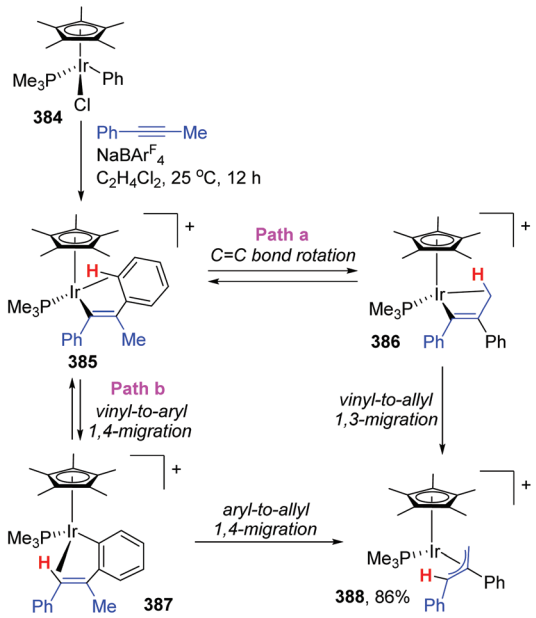

Scheme 65 1,3- and 1,4-Ir migrations in a Cp*Ir(III) complex.

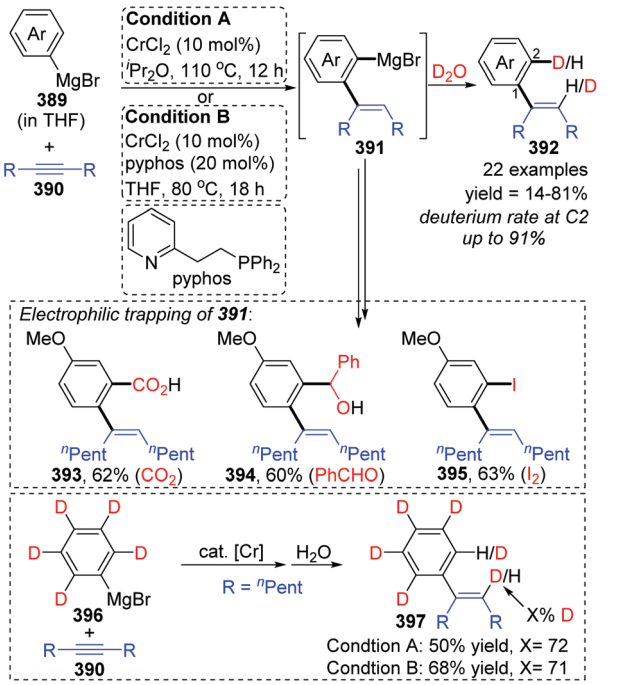

Scheme 66 Yoshikai's Cr-catalyzed reaction of arylmagnesium bromides with unactivated internal alkynes.

Both of the pathways were strongly supported by deuterium labeling experiments. Overall, this reaction provided the first experimental evidence of formal 1,3-metal migration accompanied by C–H bond activation, which was of great significance for the future metal migration strategies.

7 Chromium migration

In 2017, Yan and Yoshikai described a chromium-catalyzed addition reaction of an arylmagnesium bromide **389** to an unactivated internal alkyne **390**, affording the *ortho*-alkenylarylmagnesium bromide **391** *via* alkenyl-to-aryl 1,4-chromium migration (Scheme 66).[52] This transformation performed smoothly at almost the same level under the two reaction conditions, and the reaction was allowed to proceed at relatively low temperature (80 °C) by using the pyphos as a ligand (condition B), while the ligand-free condition was 110 °C (condition A). Reactions quenched with D_2O provided various C2-deuterated adducts **392**. Arylmagnesium bromides possessing an electron-donating group had good performance in this transformation, while employment of alkynes **390** with different substituents at both ends resulted in quite low yields. Furthermore, a series of electrophilic trapping regents, such as CO_2 and PhCHO, worked well to provide the corresponding products in moderate yields (**393** to **395**). Pentadeuteriophenylmangesium bromide **396** underwent the standard reactions to give target product **397** with high deuteration rate at the vinyl portion, which should result from 1,4-chromium shift. The proposed reaction pathway is demonstrated in Scheme 67. This conversion started with the generation of an arylchromium species **398** from the chromium precatalyst and Grignard reagent. Subsequent insertion of the

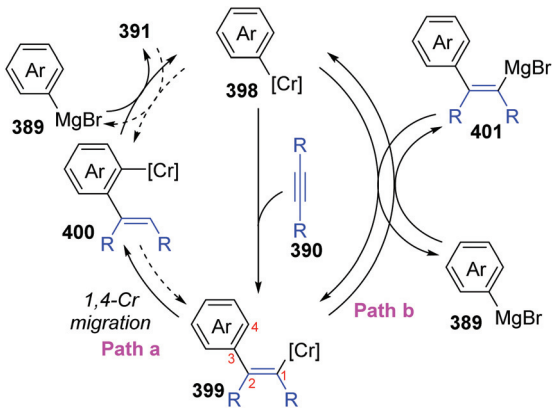

Scheme 67 Possible reaction pathways for the reaction of arylmagnesium bromides with internal alkynes.

alkyne **390** formed an alkenylchromium complex **399**, which further afforded an *ortho*-alkenylarylchromium species **400** *via* 1,4-chromium migration (path a). Final transmetalation with the arylmagnesium bromide furnished the crucial *ortho*-alkenylarylmagnesium bromide **391** with concomitant regeneration of the arylchromium species **398**. In consideration of incomplete 1,4-migration observed in product **392**, the reversible process of direct transmetalation between alkenylchromium species **399** and Grignard reagent **389** (path b) should be present to compete with the 1,4-Cr shift, which accounted for the formation of normal products **401**.

The above is the only example towards chromium migration; however, it revealed attractive resemblances com-

pared with the 1,4-cobalt migration[46] reported by the same team in 2012 (see the section on Cobalt migration). From these resemblances we can suppose that if metal-migration occurred in other Co-catalyzed reactions, it could also take place in Cr-catalyzed transformations, which needs to be verified in the future.

8 Nickel migration

One case of nickel-migration was observed in isomerizing the aryne complex **402** into the biaryl complex **403** from Johnson's report.[53] As shown in Scheme 68, the aryne complex **402** reacted with a catalytic amount of $Br_2Ni(PEt_3)_2$ over 1% Na/Hg to afford the dinuclear Ni(I) biaryl complex **403** *via* a combination of C–C bond formation and C–H bond rearrangement. Compound **404** was supposed to be formed initially from **402** under catalysis, which turned into a proposed intermediate **405** by Ni–Ni bond homolysis and 1,4-shift owing to the thermodynamic instability. Direct 1,4-shift of Ni_b and H_a could furnish the final biaryl complex **403** immediately; however, the concentration of an alternative product, **406**, generated from **405** *via* 1,4-shift of Ni_a and H_a (or Ni_b and H_b), was double that of **403** early in the reaction. Hence, complex **406** should be an intermediate corresponding to kinetics. The reversibility of the reactions allowed complex **406** to be converted into the more stable product **403** completely in approximately 48 h. The potential possibility of applying a nickel-migration strategy to practical synthetic reactions is revealed by Johnson's findings.

9 Platinum migration

A 1,4-migration of platinum and palladium at the edge of dibenz[*a*,*c*]anthracene was reported by Sharp and Singh.[54] The

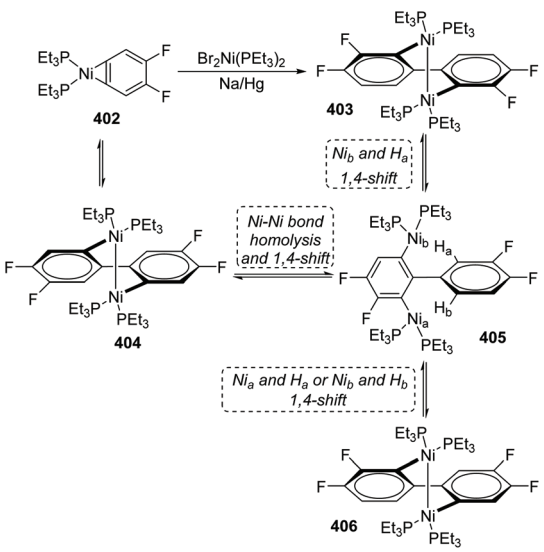

Scheme 68 Johnson's synthesis of a dinuclear Ni(I) biaryl complex *via* a 1,4-Ni shift.

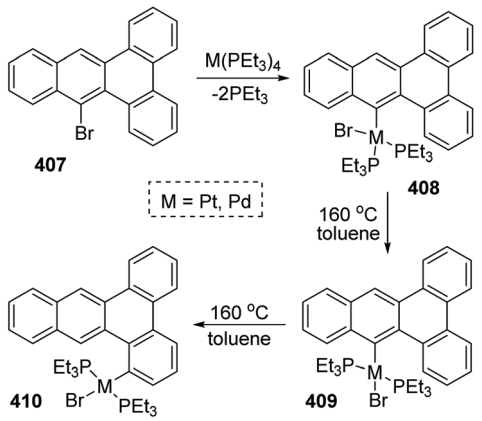

Scheme 69 Metal-migration at the edge of dibenz[*a*,*c*]anthracene.

established process of metal migration by isolating metal complexes is illustrated in Scheme 69. When the intermediate **408** in toluene solution in a sealed-tube was heated at 160 °C, it would isomerize into *trans* complex **409**. This transposition of a Br atom was supposed to alleviate the intense steric strain derived from the two PEt_3 groups. After the isomerization was

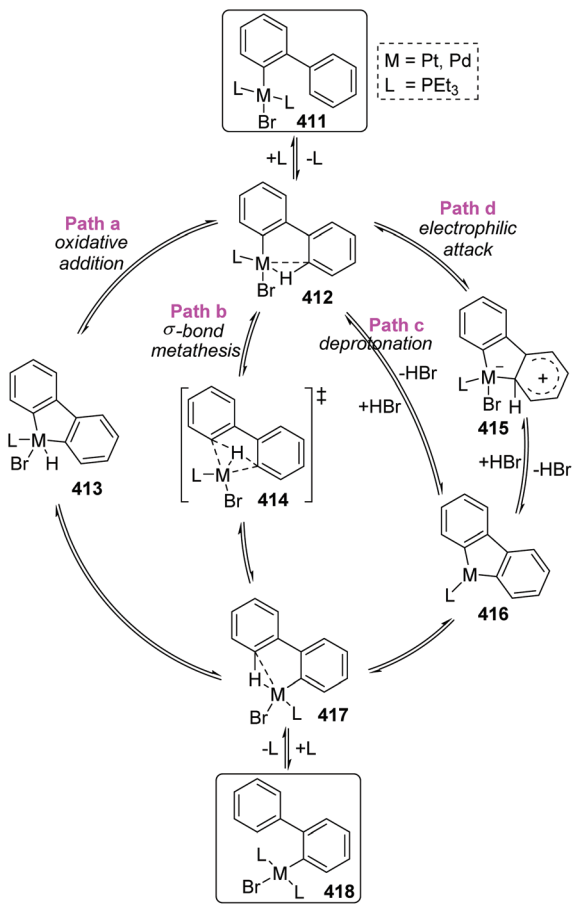

Scheme 70 Proposed mechanistic pathways for 1,4-migration on dibenz[*a*,*c*]anthracene.

nearly completed, the concentration of **409** began to drop off, accompanied by the emergence and increase of a new migratory product **410**. By comparing the structures of **409** and **410**, it was revealed that the less constrained structure of **410** might account for the greater stability than **409**, which was also responsible for the 1,4-migratory behavior of metal groups.

In Scheme 70, the abbreviated **411** was taken as an example to reveal the mechanistic pathways considered for 1,4-migration. The initial pre-agostic C–H of the phosphine ligand would change into a full-agostic and furnish the intermediate **412**. There were several possible routes that could account for the final complex **418**, such as oxidative addition of an aryl C–H bond to Pd(II) (path a), σ-bond metathesis (path b), deprotonation of an acidic agostic C–H (path c), or electrophilic attack of metal to aryl (path d). However, the deuterium scrambling experiments ruled out any possibility of path c and path d, because no deuteration was observed. Additionally, this migration process was promoted by polar solvents; therefore path b was the most possible reaction pathway and might have significant proton-transfer character.

10 Conclusions

This review has summarized the recent advances in transition-metal-migration involving reactions. To make the reader understand this field easily and deeply, most of the reaction mechanisms have been discussed in detail. Compared with relatively well-studied 1,4-palladium and 1,4-rhodium migration chemistry, other types of metal-migration reactions are just beginning to be studied, and most of the transition states have not been found or demonstrated. In addition, the migrations of nickel and platinum are only found in metal complexes and are not applied in practical methodologies. However, regularity of migration can still be observed from Pd- and Rh-migration strategies, providing theoretical help for other metal-migration protocols. In most cases, the metal atom coordinated with the ligands tends to shift to the position with less steric hindrance. Hence, the migration of transition-metals is more likely driven by intramolecular steric hindrance effects, for instance, the inherent spatial tension on a molecular level, or ligands with large steric hindrance may facilitate the migration process. Additionally, some experimental results involving Pd-migration strategies also revealed that the palladium atom tends to migrate to a more acidic position;[55] in other words, the migration site is related to the acidity of the C–H bond. Metal-migration is considered a reversible process in many mechanistic diagrams, which is supported by extensive experimental evidence. Additionally, other competing paths, in particular irreversible β-X (X = O, N, F, *etc.*) elimination against 1,4-metal migration, should also be considered. Metal-migration chemistry would be promoted significantly if further migratory experimental data and details of transition states were obtained. Moreover, the application of metal-migration strategies in the total synthesis of natural products and pharmaceuticals is also worthy of further exploration. Overall, although many transition metals have only been used in metal migration strategies, the feasibility of using migration in synthetic chemistry has also been proved. Thus, the development and prospects of the metal migration field appear to be very promising, and we can expect to see many more reports involving new methodologies soon.

Conflicts of interest

There are no conflicts to declare.

Acknowledgements

H. L. is grateful for the support from the Shandong Provincial Natural Science Foundation (ZR2018MB008, ZR2018MB012), Youth Innovative Talents Attracting and Cultivating Plan of Colleges and Universities in Shandong Province, the National Natural Science Foundation of China (21671121), and the Shandong Provincial Key Research and Development program of China (2017GGX20131).

Notes and references

1 (*a*) J.-Q. Yu, *Catalytic Transformations via C–H activation, Science of Synthesis*, Georg Thieme Verlag KG, Stuttgart, 2015, vol. 1 and 2; (*b*) J. F. Hartwig, Evolution of C–H bond functionalization from methane to methodology, *J. Am. Chem. Soc.*, 2016, **138**, 2–24.
2 S. Ma and Z. Gu, 1,4-Migration of rhodium and palladium in catalytic organometallic reactions, *Angew. Chem., Int. Ed.*, 2005, **44**, 7512–7517.
3 F. Shi and R. C. Larock, *Remote C–H activation via through-space palladium and rhodium migrations*, Springer, Berlin, Heidelberg, 2009, pp. 123–164.
4 A. Rahim, J. Feng and Z. Gu, 1,4-Migration of transition metals in organic synthesis, *Chin. J. Chem.*, 2019, **37**, 929–945.
5 T. Kochi, S. Kanno and F. Kakiuchi, Nondissociative chain walking as a strategy in catalytic organic synthesis, *Tetrahedron Lett.*, 2019, **60**, 150938.
6 A. T. Lindhardt, T. M. Gøgsig and T. Skrydstrup, Studies on the 1,2-migrations in Pd-catalyzed Negishi couplings with JosiPhos ligands, *J. Org. Chem.*, 2009, **74**, 135–143.
7 (*a*) J.-P. Ebran, A. L. Hansen, T. M. Gøgsig and T. Skrydstrup, Studies on the Heck reaction with alkenyl phosphates: can the 1,2-migration be controlled? Scope and limitations, *J. Am. Chem. Soc.*, 2007, **129**, 6931–6942; (*b*) A. L. Hansen, J.-P. Ebran, M. Ahlquist, P.-O. Norrby and T. Skrydstrup, Heck coupling with nonactivated alkenyl tosylates and phosphates: examples of effective 1,2-migrations of the alkenyl palladium(II) intermediates, *Angew. Chem., Int. Ed.*, 2006, **45**, 3349–3353.

8 E. A. Filatova, A. V. Gulevskaya, A. F. Pozharskii and V. A. Ozeryanskii, Synthesis and some properties of alkynyl derivatives of 1,3-dialkylperimidones. An example of the 1,2-palladium migration in the Sonogashira reaction, *Tetrahedron*, 2016, **72**, 1547–1557.

9 G. Yue, Y. Wu, C. Wu, Z. Yin, H. Chen, X. Wang and Z. Zhang, Synthesis of 2-arylindoles by Suzuki coupling reaction of 3-bromoindoles with hindered benzoboronic acids, *Tetrahedron Lett.*, 2017, **58**, 666–669.

10 P. M. Kathe and I. Fleischer, Palladium-catalyzed tandem isomerization/hydrothiolation of allylarenes, *Org. Lett.*, 2019, **21**, 2213–2217.

11 H. Pang, D. Wu, H. Cong and G. Yin, Stereoselective palladium-catalyzed 1,3-arylboration of unconjugated dienes for expedient synthesis of 1,3-disubstituted cyclohexanes, *ACS Catal.*, 2019, **9**, 8555–8560.

12 C.-M. Chou, I. Chatterjee and A. Studer, Stereospecific palladium-catalyzed decarboxylative $C(sp^3)$–$C(sp^2)$ coupling of 2,5-cyclohexadiene-1-carboxylic acid derivatives with aryl iodides, *Angew. Chem., Int. Ed.*, 2011, **50**, 8614–8617.

13 Z.-Y. Gu, X. Wang, J.-J. Cao, S.-Y. Wang and S.-J. Ji, Chemoselective Pd-catalyzed isocyanide insertion reaction of enaminones by C–H functionalization: hydrolysis or cyclization through 1,3-palladium migration, *Eur. J. Org. Chem.*, 2015, 4699–4709.

14 P. Jiang, Y. Xu, F. Sun, X. Liu, F. Li, R. Yu, Y. Li and Q. Wang, Pd(II)-catalyzed *ortho*-C–H olefination/dearomatization of *N*-aryl ureas: an approach to imine derivatives, *Org. Lett.*, 2016, **18**, 1426–1429.

15 B.-S. Zhang, Y. Li, Z. Zhang, Y. An, Y.-H. Wen, X.-Y. Gou, S.-Q. Quan, X.-G. Wang and Y.-M. Liang, Synthesis of C4-aminated indoles via a catellani and retro-Diels–Alder strategy, *J. Am. Chem. Soc.*, 2019, **141**, 9731–9738.

16 Q. Wang, R. Chen, J. Lou, D. H. Zhang, Y.-G. Zhou and Z. Yu, Highly regioselective C–H alkylation of alkenes through an aryl to vinyl 1,4-palladium migration/C–C cleavage cascade, *ACS Catal.*, 2019, **9**, 11669–11675.

17 M.-Y. Li, P. Han, T.-J. Hu, D. Wei, G. Zhang, A. Qin, C.-G. Feng, B. Z. Tang and G.-Q. Lin, Suzuki-Miyaura coupling enabled by aryl to vinyl 1,4-palladium migration, *iScience*, 2020, 100966.

18 T. Tsuda, Y. Kawakami, S.-M. Choi and R. Shintani, Palladium-catalyzed synthesis of benzophenanthrosilines by C–H/C–H coupling through 1,4-palladium migration/alkene stereoisomerization, *Angew. Chem.*, 2020, **59**, 8057–8061.

19 Z.-Y. Gu, C.-G. Liu, S.-Y. Wang and S.-J. Ji, Pd-catalyzed intramolecular Heck reaction, $C(sp^2)$–H activation, 1,4-Pd migration, and aminopalladation: chemoselective synthesis of dihydroindeno[1,2,3-*kl*]acridines and 3-arylindoles, *Org. Lett.*, 2016, **18**, 2379–2382.

20 M. Catellani, F. Frignani and A. Rangoni, A complex catalytic cycle leading to a regioselective synthesis of *o,o*'-disubstituted vinylarenes, *Angew. Chem., Int. Ed. Engl.*, 1997, **36**, 119–122.

21 A. J. Rago and G. Dong, Unexpected *ortho*-Heck reaction under the Catellani conditions, *Org. Lett.*, 2020, **22**, 3770–3774.

22 P. Li, Q. Li, H. Weng, J. Diao, H. Yao and A. Lin, Intramolecular remote C–H activation via sequential 1,4-palladium migration to access fused polycycles, *Org. Lett.*, 2019, **21**, 6765–6769.

23 T. Kesharwani, A. K. Verma, D. Emrich, J. A. Ward and R. C. Larock, Studies in acyl C–H activation via aryl and alkyl to acyl "through space" migration of palladium, *Org. Lett.*, 2009, **11**, 2591–2593.

24 R. Rocaboy, I. Anastasiou and O. Baudoin, Redox-neutral coupling between two $C(sp^3)$–H bonds enabled by 1,4-palladium shift for the synthesis of fused heterocycles, *Angew. Chem., Int. Ed.*, 2019, **58**, 14625–14628.

25 Y. Yu, P. Chakraborty, J. Song, L. Zhu, C. Li and X. Huang, Easy access to medium-sized lactones through metal carbene migratory insertion enabled 1,4-palladium shift, *Nat. Commun.*, 2020, **11**, 461–469.

26 Y. Yu, L. Ma, J. Xia, L. Xin, L. Zhu and X. Huang, A modular approach to dibenzo-fused ε-lactams: palladium carbene bridging C–H activation and its synthetic application, *Angew. Chem., Int. Ed.*, DOI: 10.1002/anie.202007799.

27 C. Bour and J. Suffert, Cyclocarbopalladation: sequential cyclization and C–H activation/Stille cross-coupling in the Pd-5-exo-dig reaction, *Org. Lett.*, 2005, **7**, 653–656.

28 A. J. Mota, A. Dedieu, C. Bour and J. Suffert, Cyclocarbopalladation involving an unusual 1,5-palladium vinyl to aryl shift as termination step: theoretical study of the mechanism, *J. Am. Chem. Soc.*, 2005, **127**, 7171–7182.

29 Y. Sato, C. Takagi, R. Shintani and K. Nozaki, Palladium-catalyzed asymmetric synthesis of silicon-stereogenic 5,10-dihydrophenazasilines via enantioselective 1,5-palladium migration, *Angew. Chem., Int. Ed.*, 2017, **56**, 9211–9216.

30 N. Misawa, T. Tsuda, R. Shintani, K. Yamashita and K. Nozaki, Palladium-catalyzed intramolecular C–H arylation versus 1,5-palladium migration: a theoretical investigation, *Chem. – Asian J.*, 2018, **13**, 2566–2572.

31 J.-L. Han, Y. Qin, C.-W. Ju and D. Zhao, Divergent synthesis of vinyl-, benzyl-, and borylsilanes: aryl to alkyl 1,5-palladium migration/coupling sequences, *Angew. Chem.*, 2020, **59**, 6555–6560.

32 J. Zhou, J. He, B. Wang, W. Yang and H. Ren, 1,7-Palladium migration via C–H activation, followed by intramolecular amination: regioselective synthesis of benzotriazoles, *J. Am. Chem. Soc.*, 2011, **133**, 6868–6870.

33 (*a*) L.-C. Campeau, M. Parisien and K. Fagnou, Biaryl synthesis via direct arylation: establishment of an efficient catalyst for intramolecular processes, *J. Am. Chem. Soc.*, 2004, **126**, 9186–9187; (*b*) M. Leblanc and K. Fagnou, Allocolchicinoid synthesis via direct arylation, *Org. Lett.*, 2005, **7**, 2849–2852; (*c*) C. C. Hughes and D. Trauner, Concise total synthesis of (−)-frondosin B using a novel palladium-catalyzed cyclization, *Angew. Chem., Int. Ed.*, 2002, **41**, 1569–1572.

34 Y. Wang, X. Dong and R. C. Larock, Synthesis of naturally occurring pyridine alkaloids via palladium-catalyzed coupling/migration chemistry, *J. Org. Chem.*, 2003, **68**, 3090–3098.
35 J. Zhang, J.-F. Liu, A. Ugrinov, A. F. X. Pillai, Z.-M. Sun and P. Zhao, Methoxy-directed aryl-to-aryl 1,3-rhodium migration, *J. Am. Chem. Soc.*, 2013, **135**, 17270–17273.
36 A. Archambeau and T. Rovis, Rhodium(III)-catalyzed allylic C(sp^3)–H activation of alkenyl sulfonamides: unexpected formation of azabicycles, *Angew. Chem., Int. Ed.*, 2015, **54**, 13337–13340.
37 N. Liu, J. Yao, L. Yin, T. Lu, Z. Tian and X. Dou, Rhodium-catalyzed expeditious synthesis of indenes from propargyl alcohols and organoboronic acids by selective 1,4-rhodium migration over β-oxygen elimination, *ACS Catal.*, 2019, **9**, 6857–6863.
38 L. O'Brien, S. N. Karad, W. Lewis and H. W. Lam, Rhodium-catalyzed arylative cyclization of alkynyl malonates by 1,4-rhodium(I) migration, *Chem. Commun.*, 2019, **55**, 11366–11369.
39 S. Guo, R. Pan, Z. Guan, P. Li, L. Cai, S. Chen, A. Lin and H. Yao, Synthesis of indole-fused polycyclics via rhodium-catalyzed undirected C–H activation/alkene insertion, *Org. Lett.*, 2019, **21**, 6320–6324.
40 A. Groves, J. Sun, H. R. I. Parke, M. Callingham, S. P. Argent, L. J. Taylor and H. W. Lam, Catalytic enantioselective arylative cyclizations of alkynyl 1,3-diketones by 1,4-rhodium(I) migration, *Chem. Sci.*, 2020, **11**, 2759–2764.
41 T. Matsuda, T. Izutsu and M. Hashimoto, Rhodium(I)-catalyzed arylative annulation of β-alkynyl ketones for preparation of fused aromatics, *Eur. J. Org. Chem.*, 2020, 306–310.
42 M. Font, B. Cendón, A. Seoane, J. L. Mascareñas and M. Gulías, Rhodium(III)-catalyzed annulation of 2-alkenyl anilides with alkynes through C–H activation: direct access to 2-substituted indolines, *Angew. Chem., Int. Ed.*, 2018, **57**, 8255–8259.
43 J. Mo, T. Müller, J. C. A. Oliveira and L. Ackermann, 1,4-Iron migration for expedient allene annulations through iron-catalyzed C–H/N–H/C–O/C–H functionalizations, *Angew. Chem., Int. Ed.*, 2018, **57**, 7719–7723.
44 N. Kimura, T. Kochi and F. Kakiuchi, Iron-catalyzed *ortho*-selective C–H alkylation of aromatic ketones with *N*-alkenylindoles and partial indolylation via 1,4-iron migration, *Asian J. Org. Chem.*, 2019, **8**, 1115–1117.
45 B. Zhou, H. Sato, L. Ilies and E. Nakamura, Iron-catalyzed remote arylation of aliphatic C–H bond via 1,5-hydrogen shift, *ACS Catal.*, 2018, **8**, 8–11.
46 B.-H. Tan, J. Dong and N. Yoshikai, Cobalt-catalyzed addition of arylzinc reagents to alkynes to form *ortho*-alkenylarylzinc species through 1,4-cobalt migration, *Angew. Chem., Int. Ed.*, 2012, **51**, 9610–9614.
47 B.-H. Tan and N. Yoshikai, Cobalt-catalyzed addition of arylzinc reagents to norbornene derivatives through 1,4-cobalt migration, *Org. Lett.*, 2014, **16**, 3392–3395.
48 J. Yan and N. Yoshikai, Cobalt-catalyzed arylative cyclization of acetylenic esters and ketones with arylzinc reagents through 1,4-cobalt migration, *ACS Catal.*, 2016, **6**, 3738–3742.
49 R. E. Ruscoe, M. Callingham, J. A. Baker, S. E. Korkis and H. W. Lam, Iridium-catalyzed 1,5-(aryl)aminomethylation of 1,3-enynes by alkenyl-to-allyl 1,4-iridium(I) migration, *Chem. Commun.*, 2019, **55**, 838–841.
50 B. M. Partridge, J. S. González and H. W. Lam, Iridium-catalyzed arylative cyclization of alkynones by 1,4-iridium migration, *Angew. Chem., Int. Ed.*, 2014, **53**, 6523–6527.
51 Y. Ikeda, K. Takano, S. Kodama and Y. Ishii, 1,4- and 1,3-Metal migration in a Cp*IrIII complex: experimental evidence of direct 1,3-metal migration, *Organometallics*, 2014, **33**, 3998–4004.
52 J. Yan and N. Yoshikai, Chromium-catalyzed migratory arylmagnesiation of unactivated alkynes, *Org. Chem. Front.*, 2017, **4**, 1972–1975.
53 A. L. Keen, M. Doster and S. A. Johnson, 1,4-Shifts in a dinuclear Ni(I) biarylyl complex: a mechanistic study of C-H bond activation by monovalent nickel, *J. Am. Chem. Soc.*, 2007, **129**, 810–819.
54 A. Singh and P. R. Sharp, Pt and Pd 1,4-shifts at the edge of dibenz[*a*,*c*]anthracene, *J. Am. Chem. Soc.*, 2006, **128**, 5998–5999.
55 M. A. Campo, H. Zhang, T. Yao, A. Ibdah, R. D. McCulla, Q. Huang, J. Zhao, W. S. Jenks and R. C. Larock, Aryl to aryl palladium migration in the Heck and Suzuki coupling of *o*-halobiaryls, *J. Am. Chem. Soc.*, 2007, **129**, 6298–6307.

